OPEN FILE REPORT

Geology, alteration mineralogy, geochemistry and volcanogenic massive-sulphide potential of the Ruttan mine area and the southern Rusty Lake volcanic belt (NTS 64B)

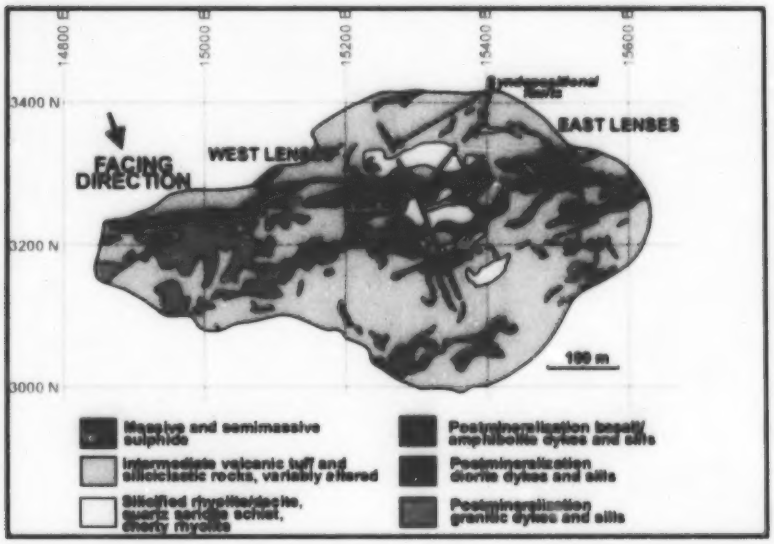

By
C.T. Barrie
and C.F. Taylor

Manitoba
Industry, Trade
and Mines

Cover:
Geology of the 4840 level of the Ruttan mine (20 m below the surface).

Georeference:
NTS area(s): 64B/5, /6, /10, /11 and /12

Keywords: alteration
anhydrite
copper ores
europium
exhalite
geochemistry
iron formations
Manitoba
massive sulphide deposits
mineralogy
modal analysis
Paleoproterozoic
petrographic norms
Ruttan
sericite
volcanic rocks
zinc ores

Suggested reference:
Barrie, C.T. and Taylor, C.F. 2001: Geology, alteration mineralogy, geochemistry and volcanogenic massive-sulphide potential of the Ruttan mine area and the southern Rusty Lake volcanic belt (NTS 64B); Manitoba Industry, Trade and Mines, Manitoba Geological Survey, Open File Report OF2001-9, 25 p. + CD-ROM.

102-01881/

Manitoba
Industry, Trade
and Mines
Manitoba
Geological Survey

Open File Report OF2001-9

Geology, alteration mineralogy, geochemistry and volcanogenic massive-sulphide potential of the Ruttan mine area and the southern Rusty Lake volcanic belt (NTS 64B)

by C.T. Barrie[1] and C.F. Taylor[2]

Winnipeg, 2001

[1] C.T. Barrie and Associates, Inc., 23 Euclid Avenue, Ottawa, Ontario K1S 2W2

[2] Hudson Bay Mining and Smelting Co. Ltd., Trout Lake Mine, Flin Flon, Manitoba R8A 1N9

Industry, Trade and Mines

Hon. MaryAnn Mihychuk
Minister

Hugh Eliasson
Deputy Minister

Mineral Resources Division

C.A. Kaszycki
Assistant Deputy Minister

Manitoba Geological Survey

E.C. Syme
Director

This publication is available in large print, audiotape or braille on request.

ABSTRACT

A review has been conducted of the geological setting, geochemistry and alteration of the Paleoproterozoic Ruttan Cu-Zn volcanic-associated massive-sulphide (VMS) mine and the Ruttan ore horizon in the southern Rusty Lake volcanic belt. The Ruttan deposit contains over 82.8 million tonnes of massive sulphide, in a series of steeply dipping lenses that extend along strike for more than 1 km at the surface and to a depth of 1 km. These lenses occur within a bimodal volcanic, volcaniclastic and siliciclastic sequence. In the immediate mine area, transitional calc-alkalic to high-silica (tholeiitic), felsic and intermediate volcanic/volcaniclastic rocks of the Mine Sequence are host to, and intercalated with, the massive-sulphide lenses. Transitional tholeiitic to calc-alkalic basalt and andesite of the Mill Pond, Vol, and Trailformations are present in the footwall sequence approximately 500 m down-section from the ore horizon. The overlying rocks of the Powder Magazine Formation are predominantly volcaniclastic and siliciclastic, but include polyfragmental agglomerate that contains mafic bombs and scoriaceous felsic fragments.

Two reconnaissance-level studies have been initiated:

1) an alteration mineralogy study on fine-grained, intermediate volcaniclastic and siliciclastic rocks that contain the Ruttan ore horizon in the southern Rusty Lake volcanic belt, with emphasis on the strata above the ore horizon
2) an examination of the metal and trace-element contents of the exhalite–sulphide/oxide-faces iron-formation (herein termed 'exhalite') that constitutes the Ruttan ore horizon, and of other exhalites, including those in the Darrol Lake trend 12 km south of the Ruttan mine, that contain the 0.6 million tonne DAR2 Cu-Zn deposit.

The purpose of these studies is to determine new and useful vectors toward significant volcanic-associated massive-sulphide mineralization in the southern Rusty Lake volcanic belt. The alteration study includes examination by X-ray diffractometry of 53 samples of intermediate rocks and 29 exhalite samples for determination of their mineralogical modes. The exhalite samples were also analyzed for their metal and trace-element contents using flux-fusion inductively coupled plasma and neutron-activation. Initial results from these studies indicate that

- the most diagnostic hydrothermal alteration minerals indicating proximity (i.e., within 200 m upsection and within 2.5 km along strike) to significant massive-sulphide deposits appear to be cordierite, anhydrite and carbonate minerals (siderite, ankerite, dolomite, calcite);
- a sericite alteration envelope to the massive-sulphide lenses at Ruttan is restricted up-section to within approximately 75 m of the upper lens; and
- at both Ruttan and Darrol Lake, the exhalites have positive Eu anomalies proximal to significant ore, whereas negative Eu anomalies are present elsewhere.

Positive Eu anomalies reflect paleoseafloor hydrothermal venting at greater than 250°C (Michard, 1989), and are considered an excellent indicator of proximity to significant base-metal deposits in the southern Rusty Lake volcanic belt.

As the regional stratigraphic section is predominantly siliciclastic, the deposit is considered most similar to bimodal-siliciclastic–type VMS deposits such as Black Mountain in the Aggeneys district of South Africa. Comparisons are also made with other very large VMS systems in the Iberian Pyrite Belt, including Neves Corvo and Rio Tinto. These comparisons suggest that there may be more ore in the immediate vicinity of the Ruttan mine.

TABLE OF CONTENTS

Page

Abstract iii
Introduction 1
Regional Geology 1
Geology of the Ruttan Mine and Darrol Lake Areas 2
Ruttan Mine Area 2
Ruttan Orebody 4
Darrol Lake Area 8
Hydrothermal Alteration: Regional X-Ray Diffraction Study 8
Regional Metal and Trace-Element Distribution along Exhalite Horizons 10
Discussion 17
Comparison with Other Large VMS Deposits and their Settings 17
Black Mountain, South Africa 17
Rio Tinto District 17
Neves Corvo 18
Fox Mine 18
Controls on Large VMS Deposits: Bulk Crustal Permeability, Crustal-Scale Faults, Magmatic Heat Source 18
Fluid Venting Temperatures and Metal Deposition 18
Heuristic Calculations: Volume of Hydrothermal Fluid Necessary to Form the Ruttan VMS Deposit 19
Role of Anhydrite in VMS Systems 19
Post-VMS Low-Temperature Venting: Regional Exhalite–Iron-Formation 20
Spacing of Crustal-Scale Hydrothermal Systems 20
Conclusions and Recommendations for Further Work 21
Recommendations 21
Acknowledgments 22
References 22

FIGURES

Figure 1: Simplified geology of the Rusty Lake volcanic belt 1
Figure 2: Geology of the Ruttan Mine area 3
Figure 3: Ruttan Mine Sequence stratigraphic area 3
Figure 4: Geology of the 4840 level of the Ruttan mine (20 m below the surface) 4
Figure 5: Plots of average continental-crust-normalized metal values for deposits listed in Table 2 6
Figure 6: Base-metal contents of massive-sulphide lenses and adjacent rocks on the 4840 level of the Ruttan mine 7
Figure 7: Longitudinal sections looking north for Ruttan mine underground workings 7
Figure 8: Darrol Lake trend with sample locations 8
Figure 9: Geology of the area around the DAR1 zone 9
Figure 10: Cross-section of the DAR2 zone at 54+00 E, looking west 9
Figure 11: Isopachs on massive sulphide, with Cu and Zn grades and relevant thickness indicated for pierce points, DAR2 zone 10
Figure 12: Typical X-ray diffraction patterns with some of the most prominent peaks labeled 11
Figure 13: Metal and trace-element contents of exhalite units along strike from the Ruttan mine 12
Figure 14: Metal and trace elements along the Darrol Lake trend 13

Figure 15: Volcanic textures in drill core and outcrops in the Ruttan mine area and southern Rusty Lake volcanic belt 14
Figure 16: Mixed magma textures in drill core and outcrops in the Ruttan mine area 15
Figure 17: Ore textures in drill core and hand samples from the Ruttan mine area 16

TABLES

Table 1: Total geological resources and mining reserves for the Ruttan mine 5
Table 2: Comparison between the Ruttan mine and other large massive sulphide deposits with 40-120 million tonnes of ore 5
Table 3: Mineralogical mode based on x-ray diffractometry for the Ruttan mine horizon and Darrol Lake horizon samples ..... on CD-ROM in back pocket
Table 4: Metal and trace-element contents for exhalite samples ..... on CD-ROM in back pocket

APPENDICES

Appendix A - X-Ray Diffraction and JADE™ Pattern-Processing Methodology 25
X-Ray Diffraction Methodology 25
JADE™ 3.1 Pattern Processing 25
Appendix B - Sample Descriptions ..... on CD-ROM in back pocket

CD-ROM

Accompanying CD-ROM has PDF and Excel files of tables 3 and 4 and Appendix B.

INTRODUCTION

The community of Leaf Rapids (population approx. 1500) is almost entirely dependent on the Ruttan Cu-Zn mine of Hudson Bay Mining and Smelting Co. Ltd. (HBMS) and its related industries for employment. The Ruttan mine has been operating nearly continuously since 1973. In October 2001, Hudson Bay Mining and Smelting Co. Ltd. announced that it will permanently close the Ruttan Mine by May 2002. The mine was scheduled to close in 2003. The company cited generally depressed mineral markets and record low commodity prices as the main reasons for the accelerated closure.

This contribution reports the initial results of an assessment of the potential for discovery of new ore reserves in the Ruttan mine area and in the southern Rusty Lake volcanic belt (RLVB). The study area comprises parts of NTS maps sheets 64B/5, /6, /10, /11 and /12. For this study, the procedure has been to

1) review the geology of the Ruttan mine and vicinity;
2) determine the potential for the discovery of new ore near the mine and along strike, based on the geology and on comparisons with other large, volcanic-associated massive-sulphide (VMS) deposits with similar characteristics, particularly other bimodal-siliciclastic–type VMS deposits; and
3) evaluate the alteration mineralogy and geochemistry of the ore horizon and nearby rocks, particularly in the strata up-section from the ore horizon, to develop new exploration criteria in this region.

This study is based on 15 days of fieldwork by the senior author and the observations of the second author, who has spent five years as a Senior Geologist and six years as the Chief Geologist at the Ruttan mine. Much of the drill core examined in this study, particularly from east of the Ruttan mine, has been recovered since 1996; thus, the observations here cover new and significant findings since the GSC–Manitoba EXTECH I program was initiated in 1989. It is anticipated that this report represents the first stage of a more comprehensive evaluation of the mineral potential of the entire Rusty Lake volcanic belt (RLVB).

REGIONAL GEOLOGY

The Rusty Lake volcanic belt (Fig. 1) is a 1.9 to 1.8 Ga greenstone belt within the Paleoproterozoic Trans-Hudson Orogen in northern Manitoba. The regional geology of the southwestern part was studied by Baldwin over a ten-year period (Baldwin, 1988). Additional descriptions of the regional geology, particularly in the southern RLVB, are provided in Speakman et al. (1982) and Ames (1996). The description of the regional geology presented here draws from these sources, and from observations of Sherritt Gordon and Hudson Bay Mining and Smelting Co. Ltd. drill core in the southern half of the belt. Baldwin (1980, 1988) viewed the RLVB as four lithologically and structurally distinct blocks, bounded by faults. Although there is some justification for considering the belt as four distinct blocks, there are several areas where volcanic and sedimentary strata carry across the fault

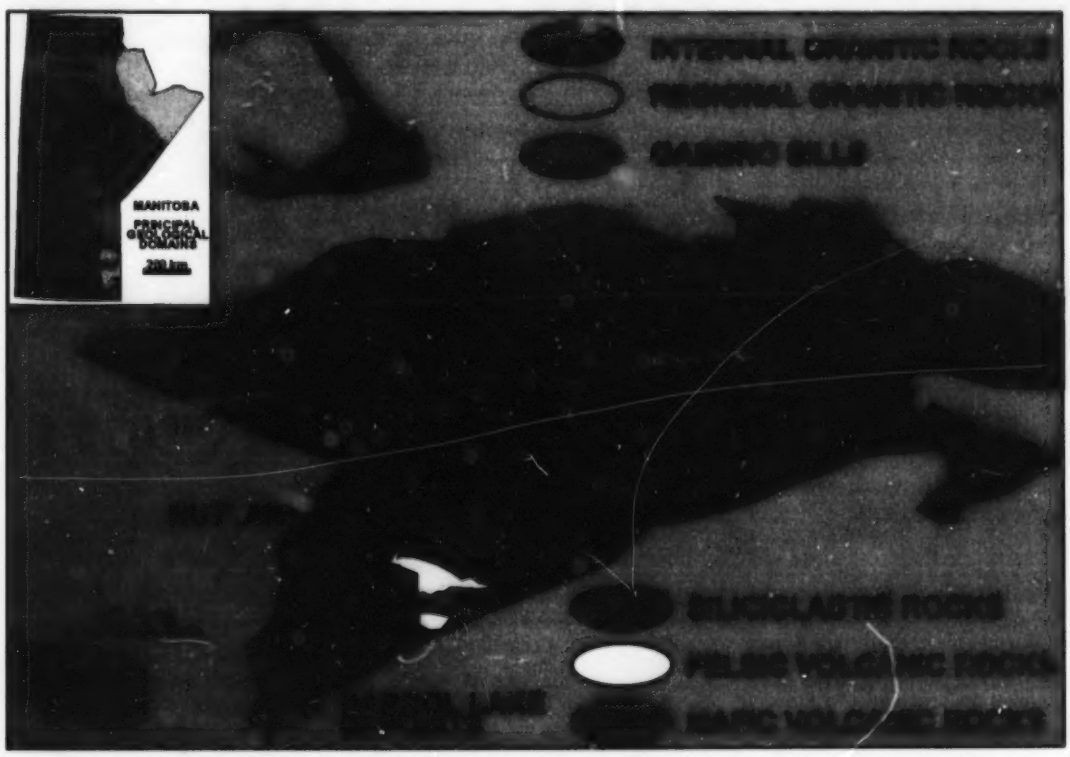

Figure 1: Simplified geology of the Rusty Lake volcanic belt, showing the locations of the Ruttan mine and the Darrol Lake deposits.

boundaries. The differences between these blocks appear to reflect facies changes in broadly coeval volcanic and sedimentary strata. Therefore, in this report, the stratigraphy of the southern RLVB is considered as one lithotectonic unit.

In broad terms, the stratigraphy of the RLVB comprises predominantly volcaniclastic and siliciclastic rocks, with subordinate mafic, intermediate and felsic volcanic rocks and mafic sills, and minor hydrothermally derived chemical sedimentary–exhalite units. To the north, 'volcanic conglomerate' and sandstone constitute well over half of the stratigraphic column, with mafic flows and gabbro sills making up most of the remainder; sulphide/oxide-facies iron-formation units, ranging from metres to tens of metres in thickness, are also present (Baldwin, 1988). The eastern quarter of the belt comprises predominantly fine-grained, intermediate volcaniclastic rocks that have been metamorphosed to upper greenschist to middle amphibolite facies; also present are mafic volcanic rocks and lesser amounts of coarse volcaniclastic rocks and exhalite–sulphide/oxide-faces iron-formation (herein termed 'exhalite'). The rocks in this area are commonly cut by intermediate to felsic dykes and sills, and are commonly strained, with gneissic, phyllic and schistose fabrics. The south-central area of the RLVB, (i.e., Baldwin's Karsakuwigamak Block, extending 5–15 km east and southeast of the Ruttan mine) contains a distinctive stratigraphic section dominated by felsic volcanic flow and tuff units. There is abundant evidence for subaerial to shallow subaqueous deposition, including units with abundant pumice and accretionary lapilli, and ignimbrite units with welding textures (Baldwin, 1988). The Ruttan mine–Darrol Lake area in the southwestern part of the belt is discussed below.

With limited exposure due to thick glacial cover, the regional structural geology of the RLVB is poorly understood. The strata to the north are predominantly north facing, and a large antiformal structure with an east-west axis is postulated to extend from 3 km north-northeast of the Ruttan mine to the east (Fig. 1). A synform may be present in the southwestern part of the belt, consisting of the south-facing Ruttan mine stratigraphy and the north-facing stratigraphy in the area of the Darrol Lake deposit; however, the core of such a synform has been largely obliterated by later intrusions. The regional metamorphic grade varies from middle greenschist to middle amphibolite facies (up to cordierite-almandine subfacies), with higher grades near the margins of the greenstone belt. Ames and Taylor (1996) documented cordierite-anthophyllite-biotite-chlorite-magnetite assemblages in the alteration immediately beneath the West Anomaly lenses of the Ruttan orebody, and determined maximum pressures of less than 400 MPa (4 kbar) and maximum temperatures of 525 to 600°C in this area.

High-quality U-Pb geochronology is nearly absent for the RLVB; the only published work is by Baldwin et al. (1987). Two samples were taken of rhyolite flows, located approximately 10 km east and along strike from the Ruttan mine. One of the two samples, R1, yielded a regression with an upper intercept at 1878 ± 3 Ma; the other sample had significantly more discordant analyses and produced a regression at 1874 +8/-7 Ma. At present, the R1 age is taken as the best estimate of the age of volcanism for the Ruttan mine section. This age is significantly younger than much of the VMS-hosting, oceanic island-arc volcanic rocks in the Flin Flon area, which are 1.91 Ga to 1.88 Ga (Stern et al., 1995; Bailes and Galley, 1996).

GEOLOGY OF THE RUTTAN MINE AND DARROL LAKE AREAS

In the southwest part of the belt, the Ruttan mine and the Darrol Lake deposits are present within a predominantly fine-grained tuffaceous, volcaniclastic and siliciclastic sequence (Fig. 1). Baldwin (1988) found similar stratigraphic sections at Ruttan, which faces south, and at Darrol Lake, which faces north. In broad terms, this region can be viewed as a synformal structure, with the core of the synform removed due to later felsic intrusive activity. In this scenario, the Darrol Lake deposits would represent nearly the same stratigraphic horizon as Ruttan. Geological maps and sections are given for Ruttan in Figures 4, 6 and 7, and for Darrol Lake in Figures 8 to 11. Additionally, outcrop and drill-core photographs of diagnostic textures of volcanic rocks, intrusive rocks and ores are shown in Figures 15 to 17.

Ruttan Mine Area

A simplified geological map of the Ruttan mine area is given in Figure 2, and the stratigraphic section is given in Figure 3 (both *modified after* Ames and Taylor, 1996). In the mine area, the strata are south-facing, and dip moderately to steeply south. Siliciclastic and volcaniclastic rocks predominate, with massive and pillowed basalt and andesite of the Mill Pond, Vol and Trail formations approximately 0.5 km down-section from the ore horizon, and a relatively narrow (maximum thickness of 0.4 km) and localized band of Mine Sequence massive felsic volcanic rocks associated with the massive sulphide.

The Mill Pond formation basalt has geochemical characteristics similar to ocean-floor basalt, and there appears to be a transition to arc tholeiite and andesite up-section in the Vol and Trail formations (Ames, 1996). Ames and Taylor (1996) found that less altered rhyolite units in the Mine Sequence have relatively high silica (approx. 71–73 wt. % SiO_2), moderate to low titania (approx. 0.31–0.35 wt. % TiO_2), low to moderate Zr (approx. 130–145 ppm) and Y (approx. 25–35 ppm), and relatively low Zr/Y (approx. 4–5). These chemical characteristics indicate that the rhyolite in the Mine Sequence has a chemical signature between those of calc-alkalic and high-silica (tholeiitic) rhyolites (Lesher et al., 1986, FII to FIIIa). Although rhyolite in predominantly metasedimentary terranes may have zircon inheritance from older crustal (metasedimentary) rocks at depth, there is evidence that this may not be a factor here, as the rhyolite analyzed for U-Pb zircon geochronology 10 km along strike does not exhibit inheritance (Baldwin et al., 1987). As the Ruttan Mine Sequence rhyolite has relatively few phenocrysts, it represents liquid compositions, and the zircon geothermometer may therefore be applicable. In this case, the Mine Sequence rhyolite would have relatively low zircon saturation (liquidus) temperatures of 790 to 810°C (using the equations of Watson and Harrison [1983] and

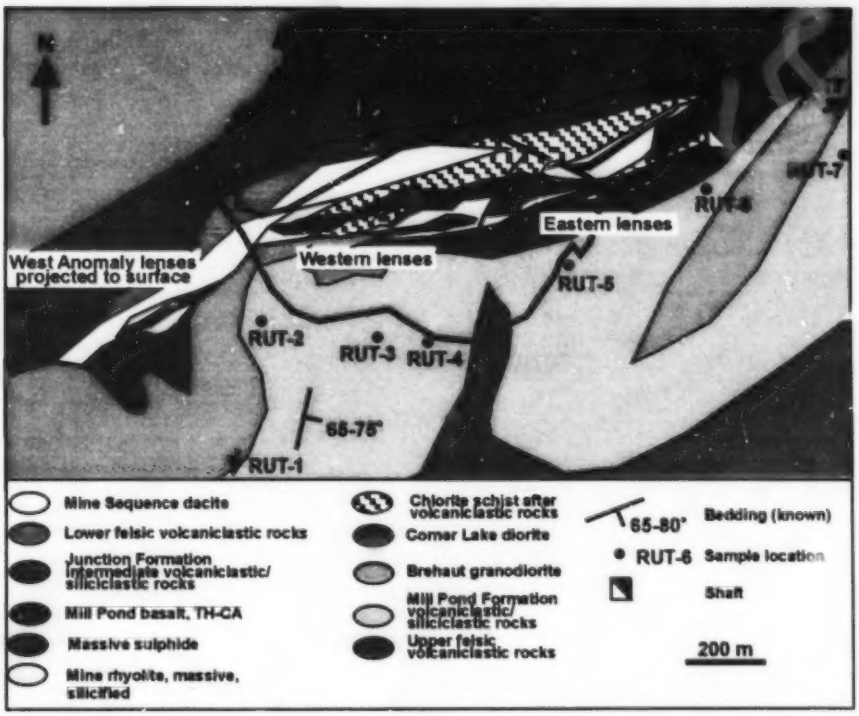

Figure 2: Geology of the Ruttan mine area, with sample locations (modified after Ames and Taylor, 1996).

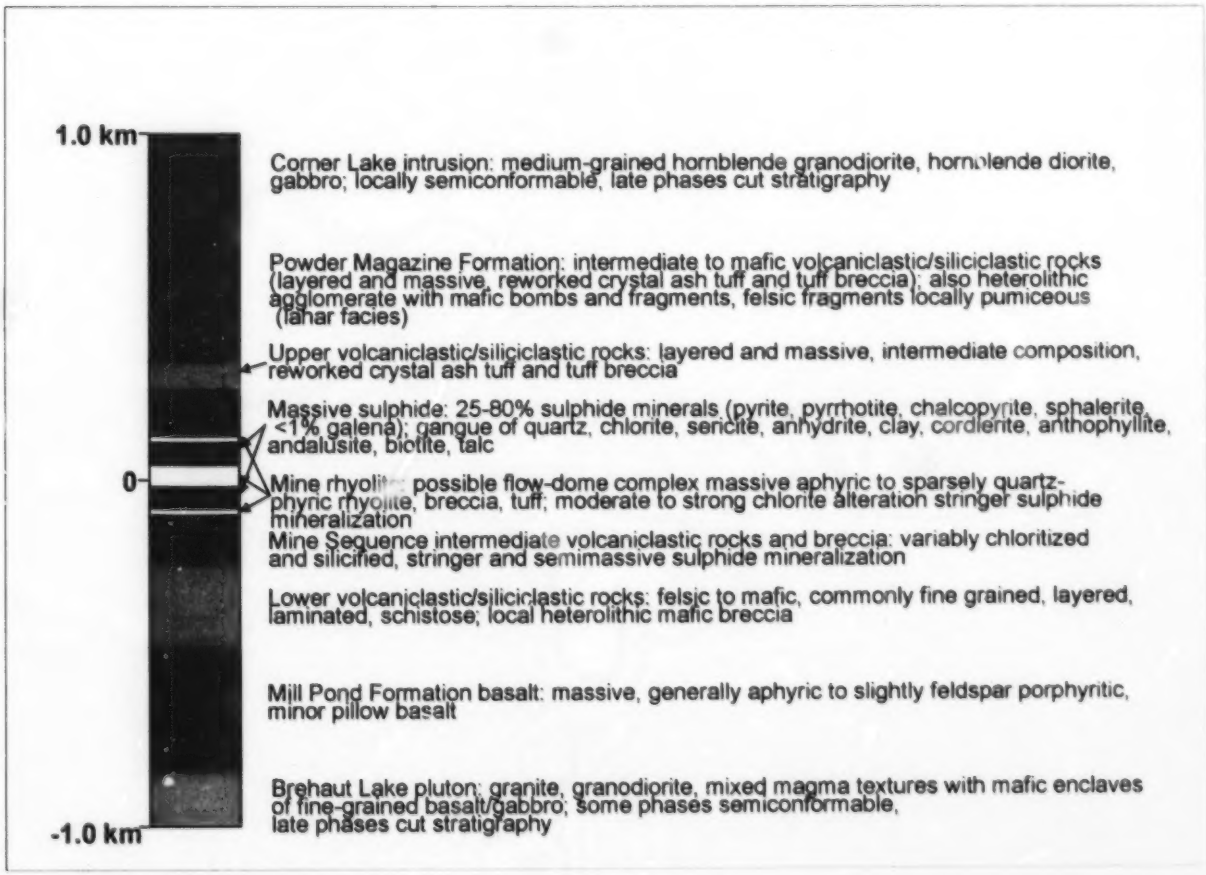
1.0 km
0
-1.0 km
Corner Lake intrusion: medium-grained hornblende granodiorite, hornblende diorite, gabbro; locally semiconformable, late phases cut stratigraphy
Powder Magazine Formation: intermediate to mafic volcaniclastic/siliciclastic rocks (layered and massive, reworked crystal ash tuff and tuff breccia); also heterolithic agglomerate with mafic bombs and fragments, felsic fragments locally pumiceous (lahar facies)
Upper volcaniclastic/siliciclastic rocks: layered and massive, intermediate composition, reworked crystal ash tuff and tuff breccia
Massive sulphide: 25-80% sulphide minerals (pyrite, pyrrhotite, chalcopyrite, sphalerite, <1% galena); gangue of quartz, chlorite, sericite, anhydrite, clay, cordierite, anthophyllite, andalusite, biotite, talc
Mine rhyolite: possible flow-dome complex massive aphyric to sparsely quartz-phyric rhyolite, breccia, tuff; moderate to strong chlorite alteration stringer sulphide mineralization
Mine Sequence intermediate volcaniclastic rocks and breccia: variably chloritized and silicified, stringer and semimassive sulphide mineralization
Lower volcaniclastic/siliciclastic rocks: felsic to mafic, commonly fine grained, layered, laminated, schistose; local heterolithic mafic breccia
Mill Pond Formation basalt: massive, generally aphyric to slightly feldspar porphyritic, minor pillow basalt
Brehaut Lake pluton: granite, granodiorite, mixed magma textures with mafic enclaves of fine-grained basalt/gabbro; some phases semiconformable, late phases cut stratigraphy

Figure 3: Ruttan Mine Sequence stratigraphic section.

Barrie [1995]). High temperature rhyolite is preferentially associated with VMS deposits in primitive volcanic terranes such as the Abitibi Subprovince (Barrie, 1995).

The Mine Sequence is cut by two intrusions, the Brehaut granodiorite to the north and west and the Corner Lake granodiorite-diorite pluton to the south. These intrusions are calc-alkalic and have similar major- and trace-element geochemical signatures (Ames and Taylor, 1996); furthermore, they are both foliated locally and are believed to have been intruded nearly synchronously, prior to much of the deformation in the area.

There are several faults in the immediate mine area, including the North Wall Shear and Art's Fault (not shown on Fig. 2), which are subparallel to the strata but do not appear to have significant displacement, and the East Shear (Speakman et al., 1982), which may be a reactivated syndepositional fault (shown on Fig. 4). Ames and Taylor (1996) noted that there is a reverse, dextral sense of displacement on the North Wall Shear. There are prominent mineral lineations (particularly in tremolite-actinolite and hornblende) and stretching lineations that plunge moderately to steeply to the east-southeast, broadly parallel to the elongation direction of the massive-sulphide lenses. A few strain indicators (e.g., amygdules, vesicles, mineral clusters) suggest that the strata have been stretched parallel to the mineral fabric and elongated by a factor of more than 25%, but this is difficult to fully assess from the few measurements taken at the surface in this reconnaissance study.

Ruttan Orebody

The Ruttan massive-sulphide orebody comprises three principal lenses or groups of lenses: the West and East lenses, which were present in the pit and are shown in Figures 2 and 4, and the West Anomaly lenses, which is entirely in the subsurface to the west, and partly below, the pit. The geology and mineralogy of these lenses have been described, in part, by Speakman et al. (1982) and Ames and Taylor (1996). This presentation focuses on total metal contents and metal zonation for the entire orebody.

The most current estimate for the geological resources for the Ruttan massive-sulphide deposit and the mining reserves for the Ruttan mine are given in Table 1. The total resource, including the open pit and underground massive-sulphide lenses, is 82.8 Mt grading 1.37 wt. % Cu, 1.63 wt. % Zn, 0.08 wt. % Pb, 0.49 g/t Au and 13.11 g/t Ag. In terms of tonnage, Ruttan ranks in the top 5% of all known VMS deposits (using data from Barrie et al., in press). In Table 2, total geological resource is compared to other VMS deposits that have 40 to 120 Mt of ore. In Figure 5, the metal contents are compared to these other deposits on

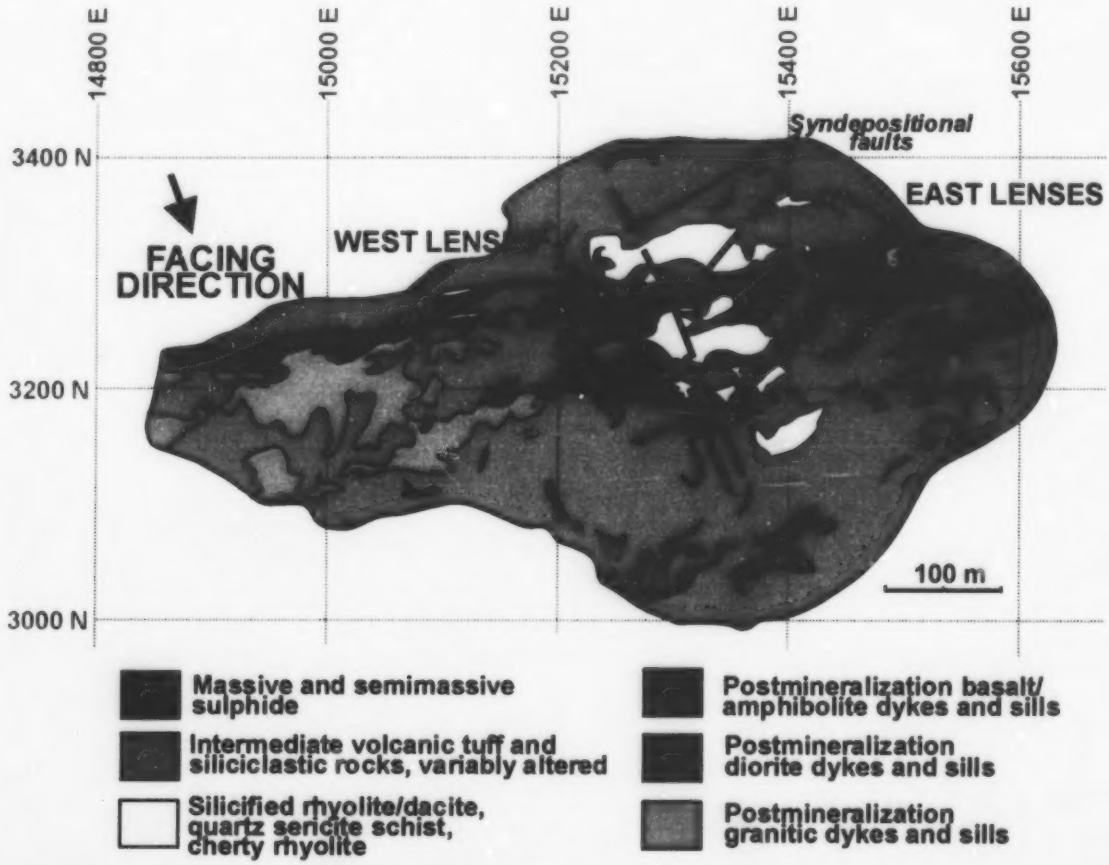

Figure 4: Geology of the 4840 level of the Ruttan mine (20 m below the surface).

Table 1: Total geological resources and mining reserves for the Ruttan mine.

Geological Resources:[1]

Area	Tonnage (t)	Cu (wt.%)	Zn (wt.%)	Pb[2] (wt.%)	Cu (t)	Zn (t)	Au[3] (g/t)	Ag[3] (g/t)
Main mine open pit[4]	15,600,000	1.28	2.04	0.09	199,000	318,000	0.49	13.59
Main mine underground	53,800,000	1.39	1.33	0.09	748,000	716,000	0.48	12.59
West Anomaly underground	13,400,000	1.42	2.37	0.05	190,000	318,000	0.52	14.66
Ruttan mine total	**82,800,000**	**1.37**	**1.63**	**0.08**	**1,137,000**	**1,352,000**	**0.49**	**13.11**

Mining Reserves:[5]

Area	Tonnage (t)	Cu (wt.%)	Zn (wt.%)	Pb[6] (wt.%)	Cu (t)	Zn (t)	Au[7] (g/t)	Ag[7] (g/t)
Mined open pit, Main mine	18,300,000	1.09	1.74	0.11	199,000	319,000	0.45	12.45
Mined underground, Main mine	29,100,000	1.30	1.04	0.07	378,000	304,000	0.46	11.76
Mined underground, West Anomaly	6,700,000	1.32	1.97	0.05	89,000	132,000	0.49	13.60
Reserve underground, Main mine	4,600,000	0.79	1.71	0.10	36,000	79,000	0.41	11.49
Reserve underground, West Anomaly	3,100,000	1.01	1.95	0.05	31,000	60,000	0.45	12.62
Total ore recovered	**61,800,000**	**1.19**	**1.45**	**0.08**	**733,000**	**894,000**	**0.46**	**12.19**

[1] includes all material identified as potentially minable, calculated using a 3-D kriged block model and based on a 1% Cu equivalent cutoff
[2] estimates based on assays but not modelled
[3] estimated from mill-head grades
[4] estimated from production reports, not modelled
[5] includes all ore mined as of January 1, 2001 and expected to be mined in the future
[6] estimated
[7] estimated using incomplete records

Table 2: Comparison between the Ruttan mine and other large massive sulphide deposits[1] with 40-120 million tonnes of ore.

Name and district	District/province and country	Tonnage (t)	Cu (wt.%)	Zn (wt.%)	Pb (wt.%)	Au (g/t)	Ag (g/t)	Age (Ma)
Bimodal-siliciclastic:								
Ruttan	**Rusty Lake Volcanic Belt, Manitoba, Canada**	**82,800,000**	**1.37**	**1.63**		**0.49**	**13.11**	**1875**
Sotiel	Iberian Pyrite Belt, Spain	41,000,000	0.62	4.27	1.34			320
Black Mountain[2]	Aggeneys District, South Africa	81,600,000	0.75	0.59	2.67		30	1980
Carthagena	Iberian Pyrite Belt, Spain	100,000,000		0.80	1.5		11	300
Masa Valverde	Iberian Pyrite Belt, Spain	100,000,000	0.50					345
Migollas	Iberian Pyrite Belt, Spain	100,000,000						345
Mafic-siliciclastic:								
Preiska	South Africa	47,000,000	1.70	3.80		0		1300
Rouez	Massif Amorican, France	90,744,102	0.60	1.50		1.5	21	600
Saladipura	Dehli Supergroup, India	112,000,000		1.00				1600
Bimodal-mafic:								
Geco	Geco District, Ontario	58,400,000	1.86	3.45	0.15		50.06	2720
Crandon	Wisconsin, USA	61,130,000	1.04	5.56	0.48	0.11	39.1	1875
Flin Flon	Flin Flon, Manitoba, Canada	62,927,000	2.20	4.10		2.85	43.2	1875
San Nicolas[2]	Zacatecas, Mexico	99,523,000	1.40	1.60		0.4	23.7	145
Harper Creek, Kamloops area	Kamloops, British Columbia, Canada	85,500,000	0.39				2.2	365
Mt. Lyell	Mt. Lyell District, Tasmania	98,574,372	1.17	0.04	0.01	0.39	7.2	495
Bimodal-felsic:								
Selbaie	Abitibi Subprovince, Quebec, Canada	44,021,245	1.05	1.98		0.47	32.13	2729
Mt. Morgan	Queensland, Australia	50,000,000	0.70	0.10	0.05	4.7	6	385
Matsumine-Shakanai	Kuroko District, Japan	54,200,000	2.19	2.63	0.76	0.62	64	15
TG-1, Tambo Grande	Piura State, N. Peru	64,200,000	1.60	1.47	0.36	0.7	30	175
TG-3, Tambo Grande[2]	Piura State, N. Peru	82,000,000	1.00	1.40		0.8	25	175
Anayatak-Cakmakkaya	Murgul District, Turkey	71,800,000	1.10	0.10	0.05	0.05	3.7	175

[1] see Barrie et al. (in press) for references
[2] closest grade-tonnage comparisons to Ruttan

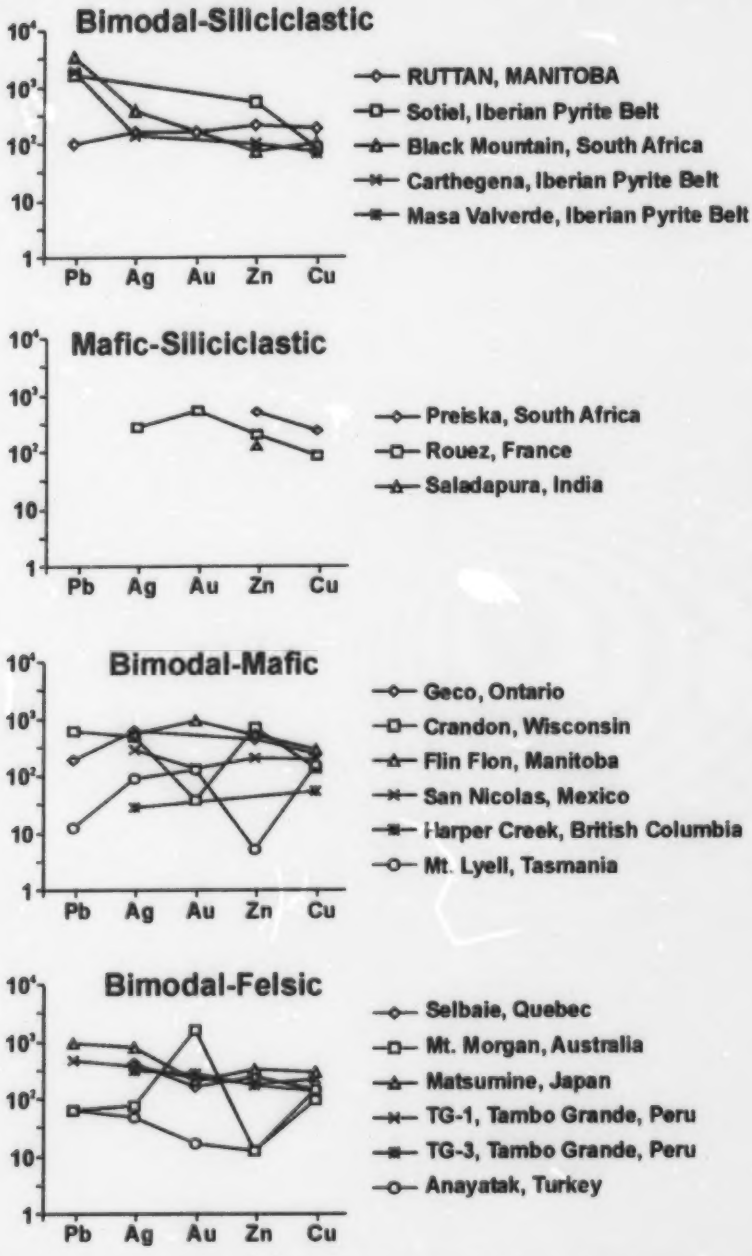

Figure 5: Plots of average continental-crust-normalized metal values for deposits listed in Table 2. Normalization values given in Barrie and Hannington, 1999.

diagrams that normalize the metal contents to average continental crust. Ruttan's metal content is 120 to 220 times that of the average continental crust, and the metals plot as a rather flat line on the diagram. Although the metals are leached at different temperatures and are affected differently by the pH of the hydrothermal fluid, this diagram may suggest that the metals were derived from crustal sources.

A geological map of the 4840 level (20 m below the surface) of the Ruttan open pit is shown in Figure 4 (*modified from* a Sherritt Gordon map). In this report, there is no distinction between the Mine Sequence dacite and rhyolite volcaniclastic rocks and the overlying Powder Magazine Formation; these distinctions are difficult to discern in drill core and at the surface, where the rocks are generally overprinted with moderate to intense chlorite-sericite alteration or chlorite-tremolite-actinolite±cordierite alteration. The massive sulphide is generally stratiform, and thickest near the rhyolite. Although the rhyolite is silicified and sericitized, it appears to have been originally a massive flow lobe in an apron of autoclastic debris, similar to rhyolite in other massive-sulphide settings where the felsic magmas have used the same conduit to the paleoseafloor as much of the hydrothermal fluids (e.g., Kuroko deposits, Kidd Creek). Mafic dykes and apophyses and blocks are present in strata below and above the massive sulphide (Fig. 4), and within massive sulphide in numerous underground locations. They are generally moderately to

highly altered and, in places within massive sulphide, intensely altered to chlorite-talc rock. Possible peperite textures are present within massive sulphide and within siliceous sedimentary material immediately above the ore (e.g., 590 level, West Anomaly lenses). This would suggest that mafic magmatism, as well as felsic magmatism, was active at the time of massive-sulphide deposition.

The base-metal contents of the massive-sulphide lenses and adjacent areas are shown in Figures 6a and b. For the 4840 level, Cu is concentrated preferentially at the base of the West lenses, and locally toward the stratigraphic top of the East lenses in the centre of the pit. Zinc is concentrated in a stratiform layer in the lower East and West lenses. In Figure 7, the entire deposit, including the underground West Anomaly lenses, is portrayed in a north-facing longitudinal section. These sections are derived from an underground mine database that has calculated average metal contents for 10 x 10 x 5 m thick (across strike) blocks for all of the known massive sulphide, including material that will not be recovered. The isopachs in Figure 7a represent the composite thickness for all sulphide with the given X (location longitudinally) and Z (depth) block co-ordinates. They were calculated using an algorithm that determines the block density from the average Fe, Cu and Zn contents, based empirically on mining-head-grade data over ten years. The calculated isopachs were cross-referenced with geological sections and found to agree to within 10%.

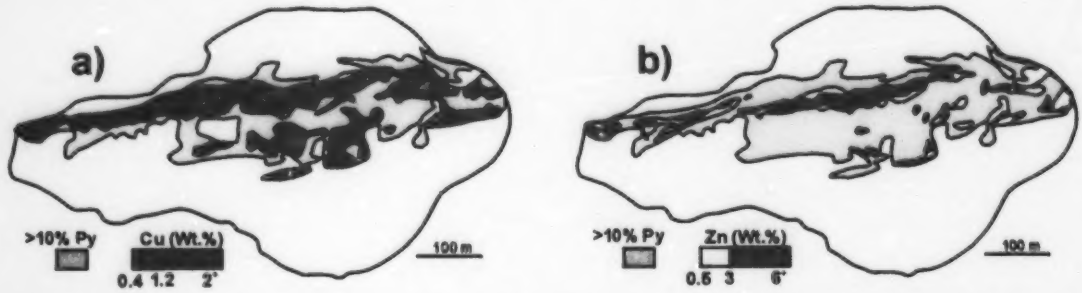

Figure 6: Base-metal contents of massive-sulphide lenses and adjacent rocks on the 4840 level of the Ruttan mine: a) contoured Cu grade; b) contoured Zn grade.

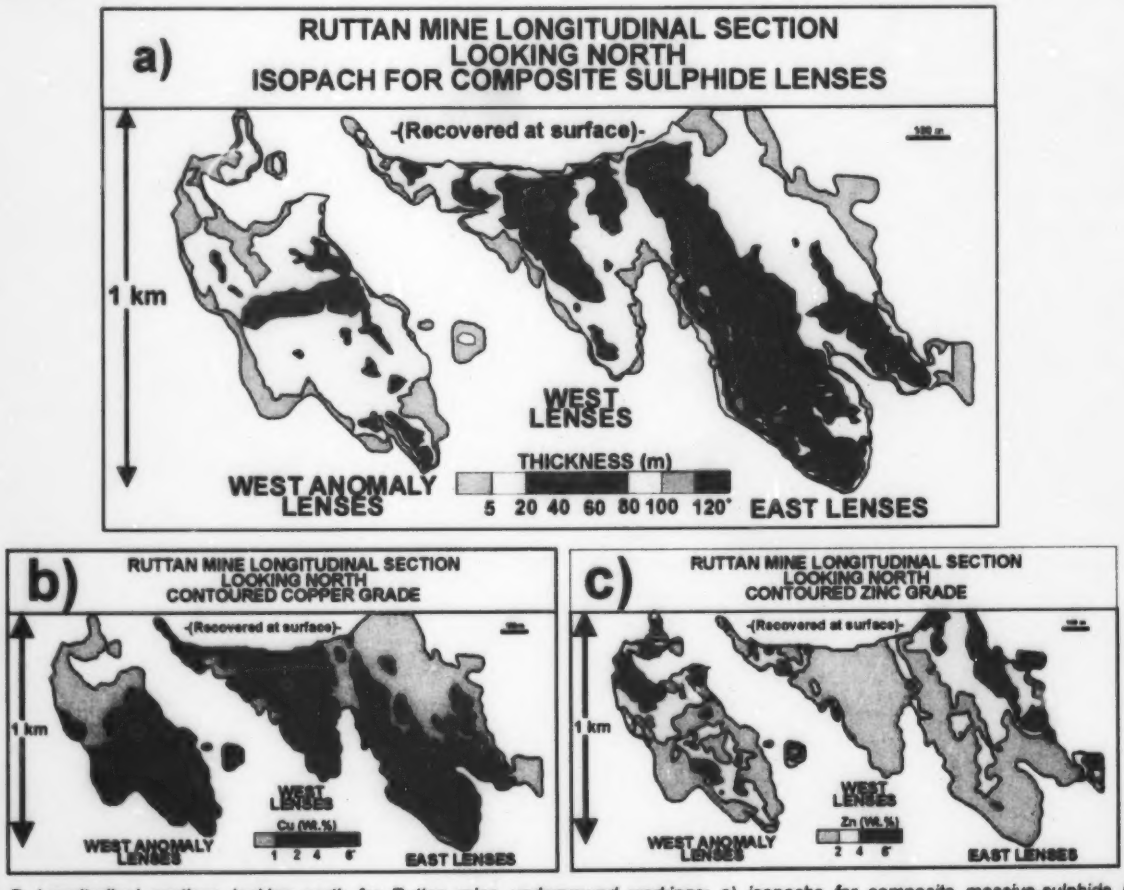

Figure 7: Longitudinal sections looking north for Ruttan mine underground workings: a) isopachs for composite massive-sulphide lenses; b) contoured Cu grade; c) contoured Zn grade. See text for discussion.

The isopachs for the massive sulphide highlight several features. In the West Anomaly lenses, there is a subhorizontal zone at approximately 500 m depth where the lens thickens. This is due to structural thickening where at a post-ore reverse fault subparallel to bedding has a displacement of several tens of metres. Of particular interest are the zones where the sulphide thickens to more than 80 m; in two locations near the western margin of the East lenses, the ore is more than 120 m thick. This is as thick as the thickest massive sulphide at the giant Kidd Creek deposit in the Abitibi Subprovince of Ontario (Hannington et al, 1999), and surpassed in Canada only by Brunswick No. 12, which is up to approximately 250 m thick in places due to structural thickening (Luff et al., 1992). The dramatic increase in thickness in sulphide adjacent to massive rhyolite suggests that 1) a graben- or half-graben–like fault was active at the time of ore deposition; and 2) the massive rhyolite may have utilized this fault to rise to the paleoseafloor, similar to other rhyolite-associated VMS deposits (e.g., Kuroko deposits, Kidd Creek, etc.).

Contoured Cu and Zn contents for the massive sulphide in the longitudinal sections do not particularly correlate with the isopachs. Higher Cu values are found in the central part of the West lenses, and in the lower half of the West Anomaly. Higher Cu values at the base of VMS deposits can point to a locus of hydrothermal venting. Given, however, that the stratigraphically higher lenses are enriched in Cu in the West lenses (Fig. 6a), another mechanism for Cu enrichment, namely zone refining, may also have been operative. Analysis and discussion of this topic are beyond the scope of this project this year. Zinc is low in the centre of the deposit and preferentially concentrated at the eastern edge, at the western edge of the West lenses area, and in the centre of the West Anomaly lenses (Fig. 6b).

Darrol Lake Area

The Darrol Lake area has four lesser Cu-Zn deposits or occurrences along a series of exhalite horizons that extend for more than 10 km along an east-northeasterly strike direction, approximately 12 km south of the Ruttan mine (Fig. 8–11). As mentioned above, the stratigraphic section is broadly similar to that found at Ruttan, with intermediate siliciclastic and volcaniclastic rocks and volcanic tuff; additionally, there are basalt/amphibolite units, and exhalite–sulphide/oxide-facies iron-formation. Rhyolite units with trace-element characteristics similar to the Mine Sequence rhyolites are present, but massive rhyolite is apparently absent. The units dip moderately to steeply north. The DAR2 zone has seen several campaigns of drilling, and at least 16 drillholes have defined a deposit with a strike length of approximately 250 m (open to the east), a depth of approximately 250 m (open at depth), thicknesses of 2 to 10 m, and a geological resource of approximately 0.61 Mt grading 0.39 wt. % Cu and 3.63 wt. % Zn (Fig. 11; Taylor, HBMS internal report, 2000). Alteration is widespread within 50 to 75 m of the iron-formation at DAR1 and DAR2, and is largely confined to intermediate volcaniclastic rocks. Tremolite-actinolite, chlorite, garnet, sericite, quartz and pyrite constitute much of the alteration assemblage, with cordierite, sillimanite and anhydrite occurring locally.

HYDROTHERMAL ALTERATION: REGIONAL X-RAY DIFFRACTION STUDY

A mineralogical study has been initiated that focuses on the Powder Magazine Formation (hanging wall) intermediate volcaniclastic rocks, and similar strata east of the Ruttan mine and in the Darrol Lake trend, 12 km south of the Ruttan mine. Recent X-ray diffraction (XRD) studies have demonstrated that variations in the mode of alteration minerals in hanging-wall strata of VMS districts, such as the Mattagami district in Québec (Ioannou et al., work in progress, 2001) and the Skellefte district

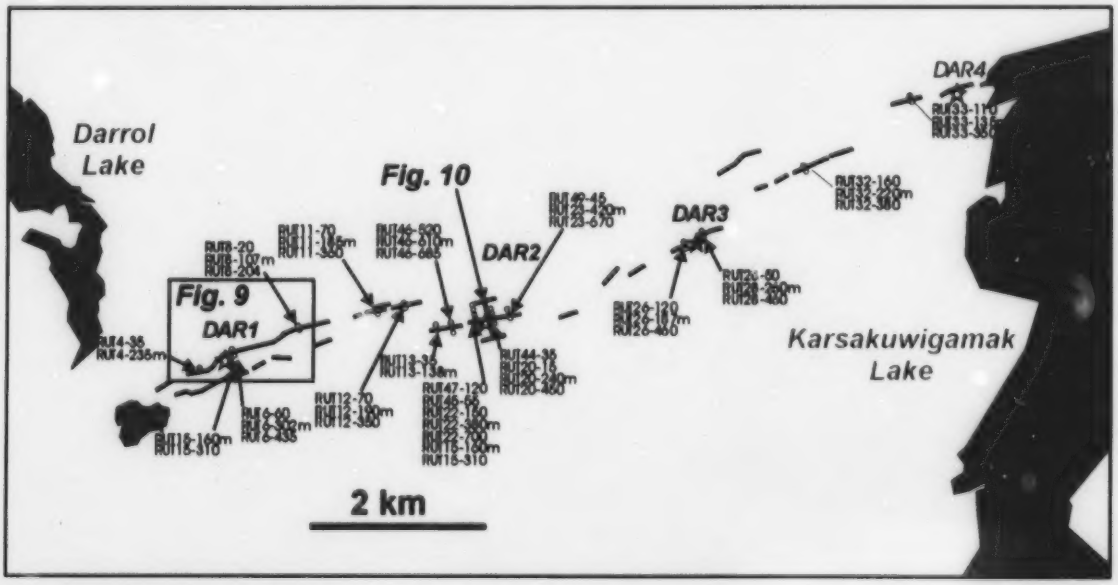

Figure 8: Darrol Lake trend with sample locations.

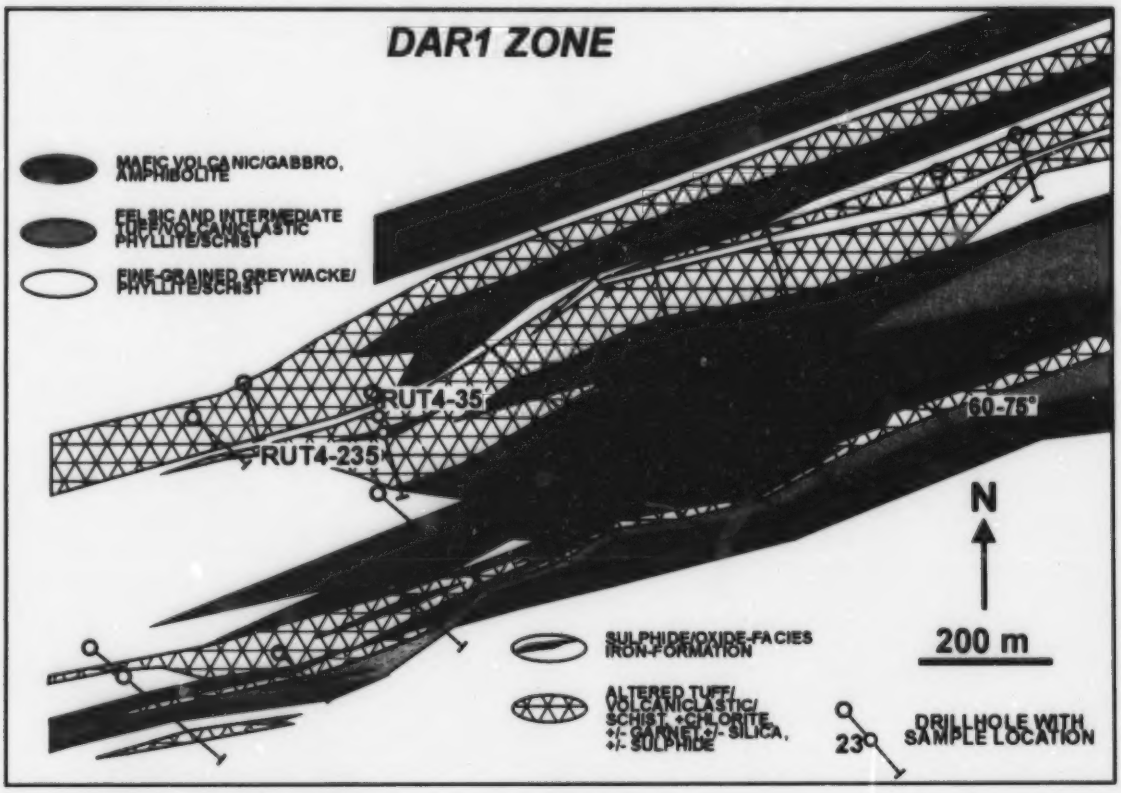

Figure 9: Geology of the area around the DAR1 zone.

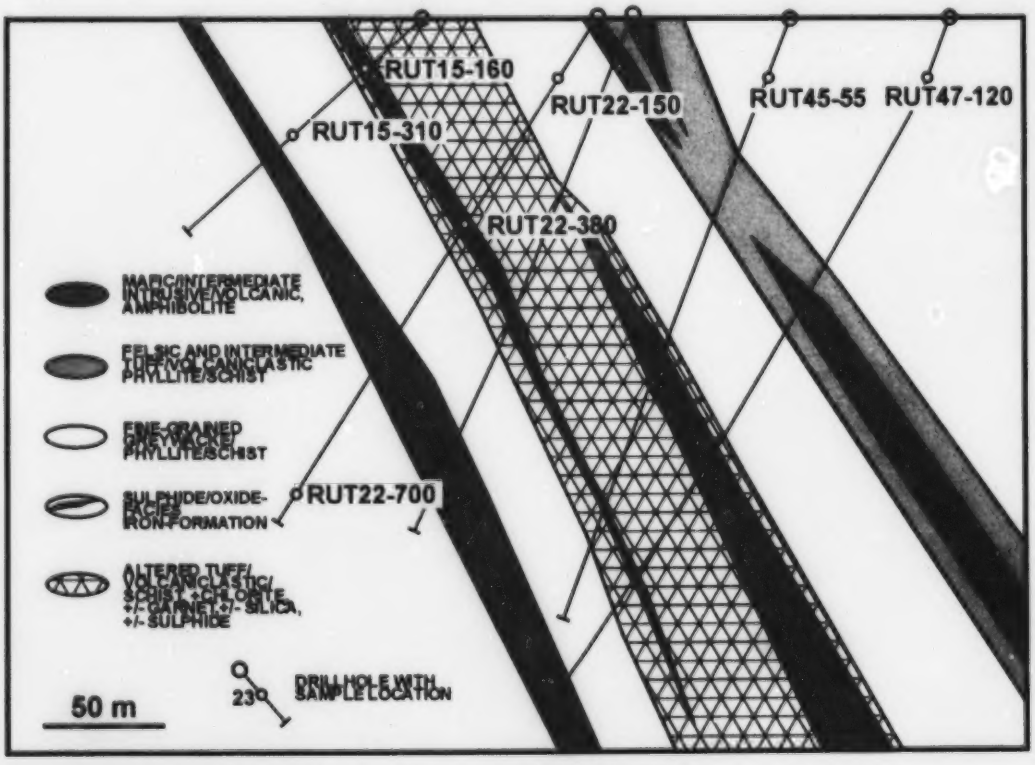

Figure 10: Cross-section of the DAR2 zone at 54+00 E, looking west. See Figure 8 for location.

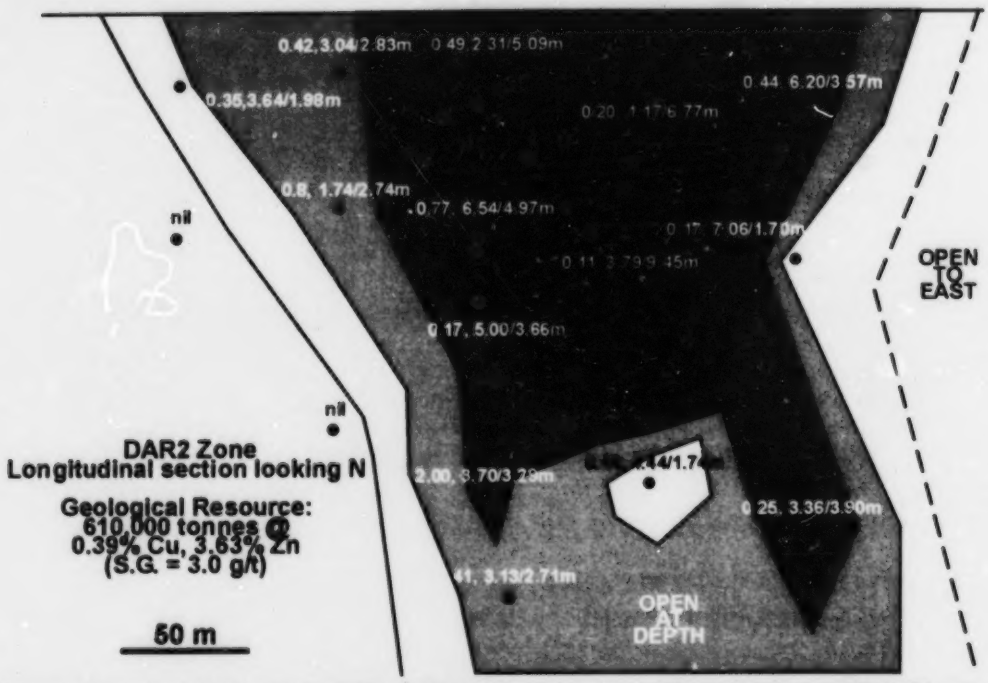

Figure 11: Isopachs on massive sulphide, with Cu and Zn grades and relevant thickness indicated for pierce points, DAR2 zone.

in Sweden (Hannington et al., work in progress, 2001), is an effective technique for outlining areas of hydrothermal alteration related to significant base-metal accumulations. For this study, 53 samples of intermediate volcaniclastic rocks have been taken, and their mineralogical modes are given in Table 3 (*see* accompanying CD-ROM). Additionally, XRD has been performed on exhalite samples taken for metal- and trace-element study (described below). Details of the XRD technique and the methodology to determine mineralogical modes using the Jade™ program, are outlined in Appendix A. All of the samples are described in Appendix B (*see* accompanying CD-ROM). Examples of the XRD patterns generated for an exhalite sample and a fine-grained intermediate phyllite are given in Figure 12.

A wide variety of minerals is found in the intermediate volcaniclastic rocks and the exhalites. They reflect a provenance from mafic, intermediate and felsic volcanic sources, hydrothermal overprinting and fallout on the paleoseafloor, and a variable metamorphic overprint in the region. The most common minerals are quartz, feldspar (including plagioclase represented as albite, and 'albite-ca' [calcic plagioclase], orthoclase and microcline), amphibole (hornblende, tremolite-actinolite, cummingtonite and edinite), garnet (including almandine, pyrope and grossular end members; possibly some spessartine as a component), clinochlore and ferroan clinochlore, muscovite, biotite, cordierite and kyanite, and sulphide minerals (pyrite, pyrrhotite, sphalerite, galena, chalcopyrite and marcasite). Lesser amounts of carbonate (including siderite, dolomite, aragonite and calcite), anhydrite, hematite, ilmenite, titanite and anatase/rutile are also present. Many of these minerals have been noted in thin section in the vicinity of the Ruttan deposit by Speakman et al. (1982) and Ames and Taylor (1996).

From this initial study, the most diagnostic minerals in terms of proximity (i.e., within 200 m up-section and within 2.5 km along strike) to significant sulphide accumulations appear to be cordierite, anhydrite and various carbonate minerals (siderite, ankerite, dolomite and calcite). Anhydrite is of particular interest because it is a prominent gangue mineral within the ore (Speakman et al., 1982; Ames and Taylor, 1996). It is commonly a distinctive, light to deep purple colour, and is prominent as fracture fillings in drill core and underground. Speakman et al. (1982) mentioned that anhydrite is found within Cu-rich lower lenses and in chloritic schist near the top of the upper lens in the central part of the deposit, whereas Ames and Taylor (1996) found anhydrite within massive-sulphide bodies, as vug fillings near the top of the East lenses, and in the hanging-wall chloritic schist. The present XRD study found anhydrite in intermediate volcaniclastic rocks 200 m up-section from the orebody, as well as proximal to two of the Darrol Lake deposits. It would appear that anhydrite is limited to the massive sulphide and to approximately 200 m up-section, although the sampling density is insufficient to determine its distribution very closely. The presence of anhydrite is unusual for pre-Paleozoic VMS deposits, and it may bear on the genesis of the deposit; this is discussed below. Further analysis of these data is currently in progress.

REGIONAL METAL AND TRACE-ELEMENT DISTRIBUTION ALONG EXHALITE HORIZONS

A study has been initiated of metal contents, and selected major- and trace-element contents, of exhalite units that extend away from the Ruttan mine, principally to the east-northeast, and of the Darrol Lake deposit trend. The distribution of metals and selected trace elements in iron-formation and exhalite units can be an effective method for vectoring toward VMS mineralization (Spry et al.,

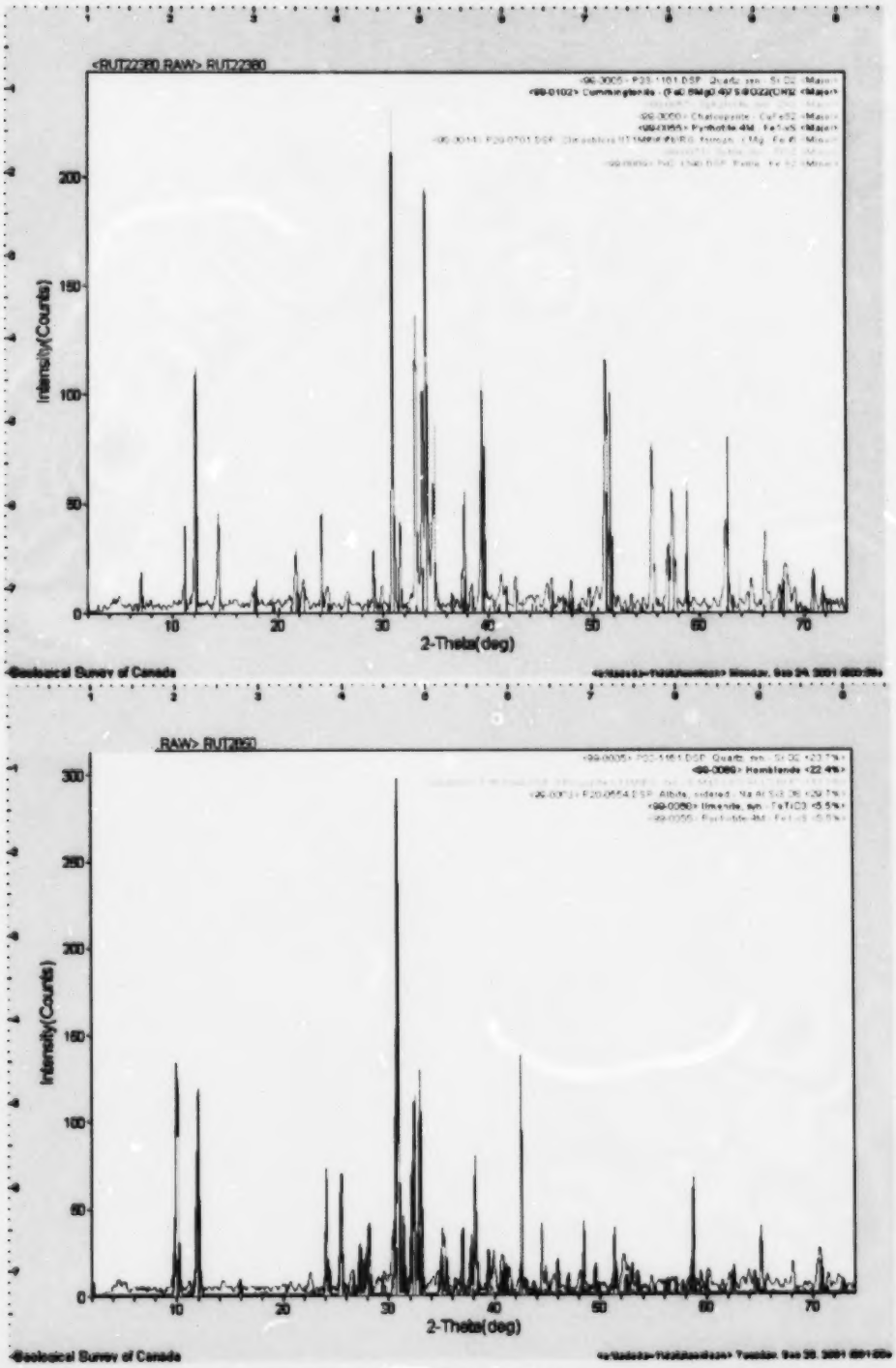

Figure 12: Typical X-ray diffraction patterns with some of the most prominent peaks labeled: a) sample RUT22-380, from semimassive sulphide adjacent to the DAR2 deposit; b) sample 28-50, from an intermediate volcaniclastic unit situated between DAR2 and DAR3. See Figure 8 for locations and Table 3 (see accompanying CD-ROM) for estimated mineralogical modes.

2001; Peter and Goodfellow, in press, and references therein). For this study, 29 samples have been taken from the surface and from drill core, and analyzed for S, Cu, Zn, Pb, Au, Ag, As, Ni, Cd, Mn; for major elements Fe and Na; and for many trace elements, including the rare-earth elements. These analyses are given in Table 4 (*see* accompanying CD-ROM). Sample locations are shown on Figures 2, 8 and 9, and their distance along strike from the centre of the Ruttan mine or the DAR2 deposit are given in Table 4. For the Ruttan exhalite horizon, the samples have been taken from outcrops immediately up-section from the mine, from outcrops extending to the east-northeast for 4.5 km, and from drill core extending up to 76 km east of the mine. For the Darrol Lake horizon, all the samples come from drill core, and from a 7.5 km total strike length.

The data that reflect important trends are presented versus strike length in Figures 13 and 14. In Figure 13, the samples near the Ruttan mine are relatively low in S, Cu, Cu/(Cu+Zn), Ni and Cr compared to the exhalite horizon(s) sampled at distance. For (Cu x 10^4)/S, the values are approximately the same for samples near and far, whereas, for (Zn x 10^4)/S, the samples near the Ruttan mine are clearly higher than those taken at a distance. Zinc normalized to S indicates a hydrothermal component derived from the Ruttan hydrothermal system. The higher Ni and Cr values at distance probably reflect a significant mafic detrital component to these exhalite samples. For the Darrol Lake trend (Fig. 14), samples come from the vicinity for the DAR1 zone (weak Cu and Zn enrichment), 2.3 to 3.0 km west of the DAR2 zone; from the DAR2 zone itself; and from areas to the west not associated with any significant mineralization. The plots of Cu, Zn, (Cu x 10^4)/S, and (Zn x 10^4)/S versus strike yield ambiguous results, whereas Cu/(Cu+Zn) highlights the DAR1 and DAR2 zones. Other metals, Pb, Au, Ag and Mn, correlate at least sporadically with the DAR1 and DAR2 zones. There is a very strong positive Eu anomaly associated with the DAR 1 zone. Furthermore, there is a weaker negative Eu anomaly associated with the DAR1 zone, suggesting that the typical negative Eu anomaly for the host rocks has been modified by the addition of Eu as a hydrothermal precipitate.

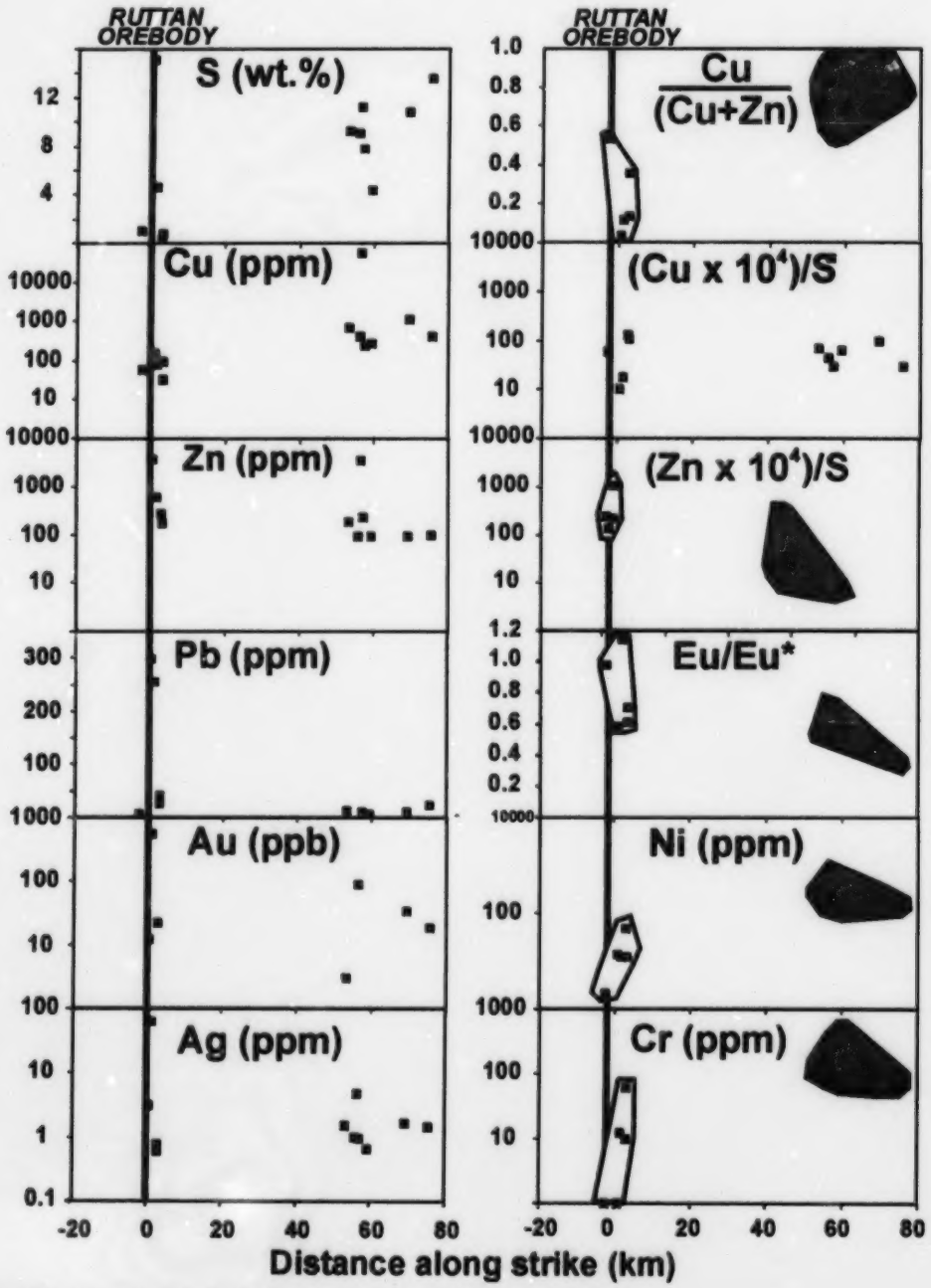

Figure 13: Metal and trace-element contents of exhalite units along strike from the Ruttan mine.

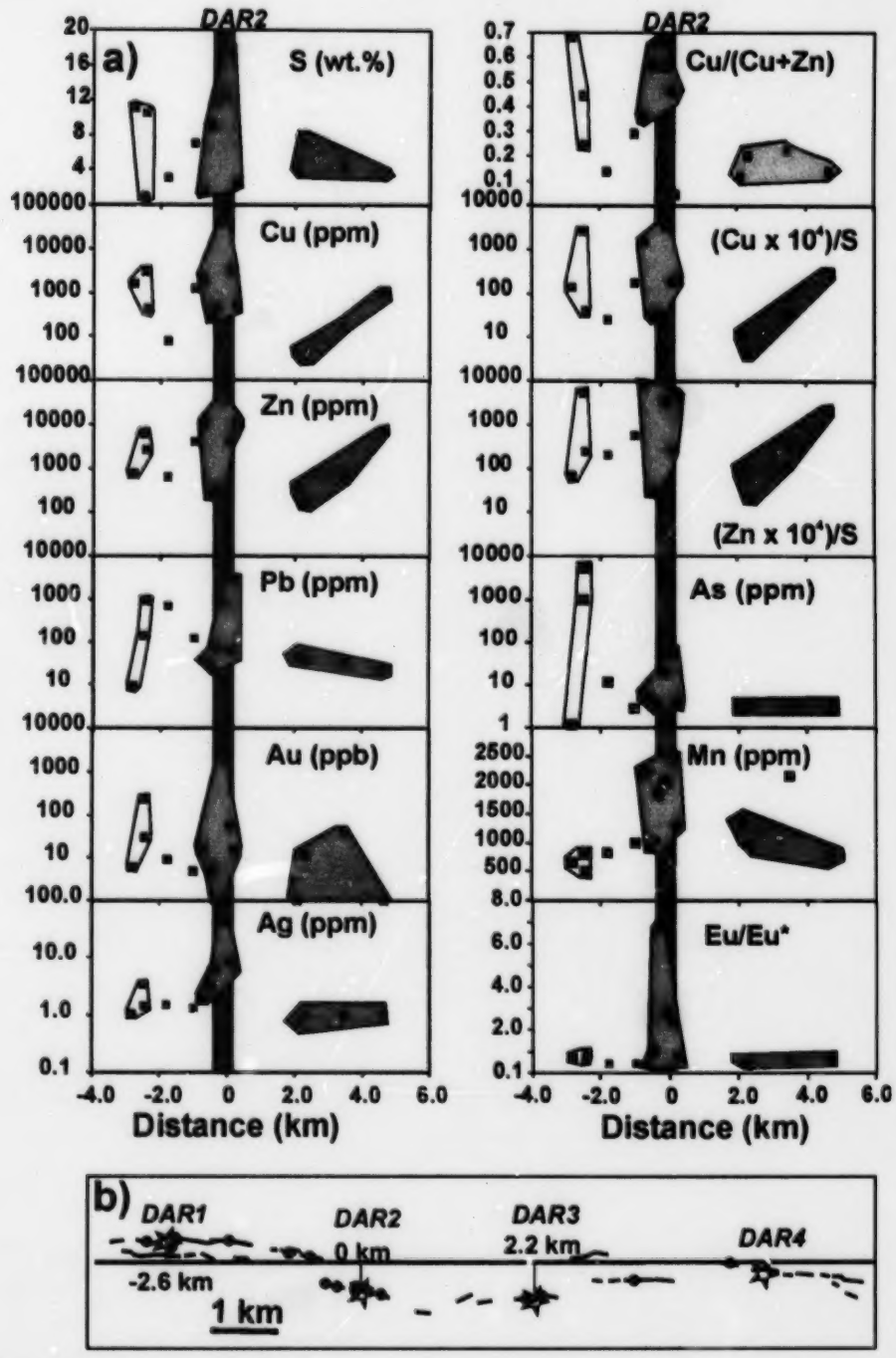

Figure 14: Metal and trace elements along the Darrol Lake trend: a) metal and trace elements versus distance along strike; b) sketch map of sample locations along trend.

Perhaps the most diagnostic element in terms of proximity to the Ruttan hydrothermal system is Eu/Eu* (chondrite normalized Eu divided by chondrite normalized Sm), which is a measure of the size of the Eu anomaly on a chondrite-normalized plot. Values of greater than one are positive Eu anomalies, which only occur in some anorthosite units and in hydrothermally derived sedimentary rocks. Europium has both +2 and +3 valence states; in the +2 state, it is relatively easily leached by acidic hydrothermal fluids at greater than 250°C during the breakdown of feldspar minerals (Michard, 1989). This has been noted in many subseafloor hydrothermal systems (e.g., Lottermoser, 1989). The Eu is then transferred preferentially through the hydrothermal system and precipitates with clay and sulphide minerals when it reaches the seafloor, and can be dispersed and deposited from a hydrothermal plume. Thus, from this pilot study, Eu/Eu* is shown to be an excellent indicator of proximity to potentially base-metal–leaching and base-metal–precipitating paleo-subseafloor hydrothermal systems in the southern RLVB.

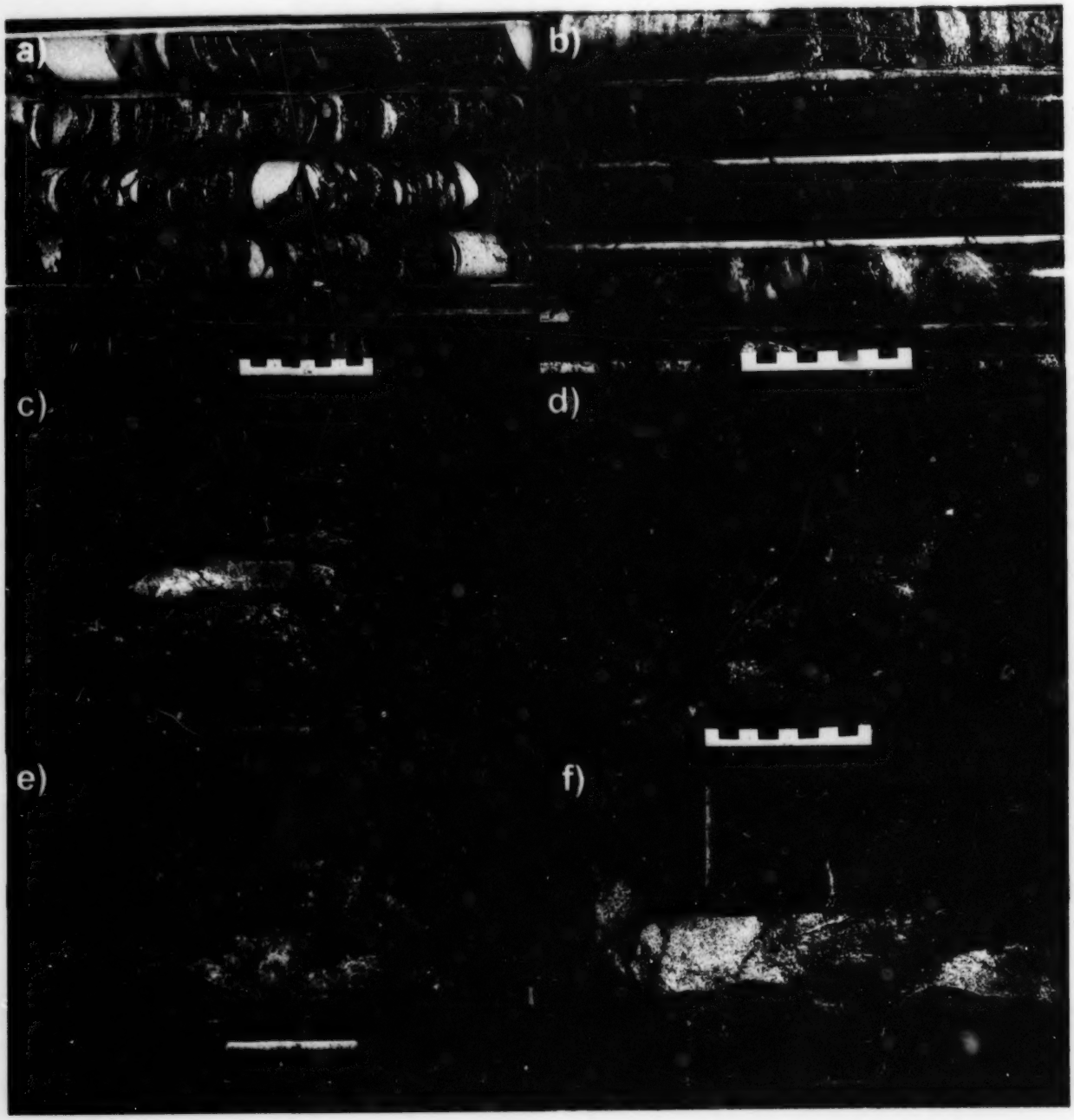

Figure 15: Volcanic textures in drill core and outcrops in the Ruttan mine area and southern Rusty Lake volcanic belt: a) heterolithic agglomerate, stratigraphically equivalent to the Powder Magazine Formation, DDH RUT75 at 30 m, 30 km east from the Ruttan mine; b) ash and crystal-ash tuff with siliceous and sulphidic exhalite, DDH RUT-75 at 60 m; c) dacite/rhyolite fragment in heterolithic agglomerate, Powder Magazine Formation, 0.7 km east of eastern edge of Ruttan pit; this agglomerate unit, >50 m thick, contains juvenile lapilli fragments and bombs of mafic and felsic composition; d) scoriaceous felsic fragment in heterolithic agglomerate, same outcrop as Figure 15c; abundant gas cavities are present in approx. 10% of the fragments in the outcrop; this unit may represent a lahar; e) juvenile mafic bomb with pigtails in heterolithic agglomerate, Powder Magazine Formation, 100 m southwest of Ruttan pit; f) felsic dyke and sill cutting Powder Magazine Formation, same outcrop as Figure 15e; felsic magma reached level of neutral buoyancy and branched subhorizontally.

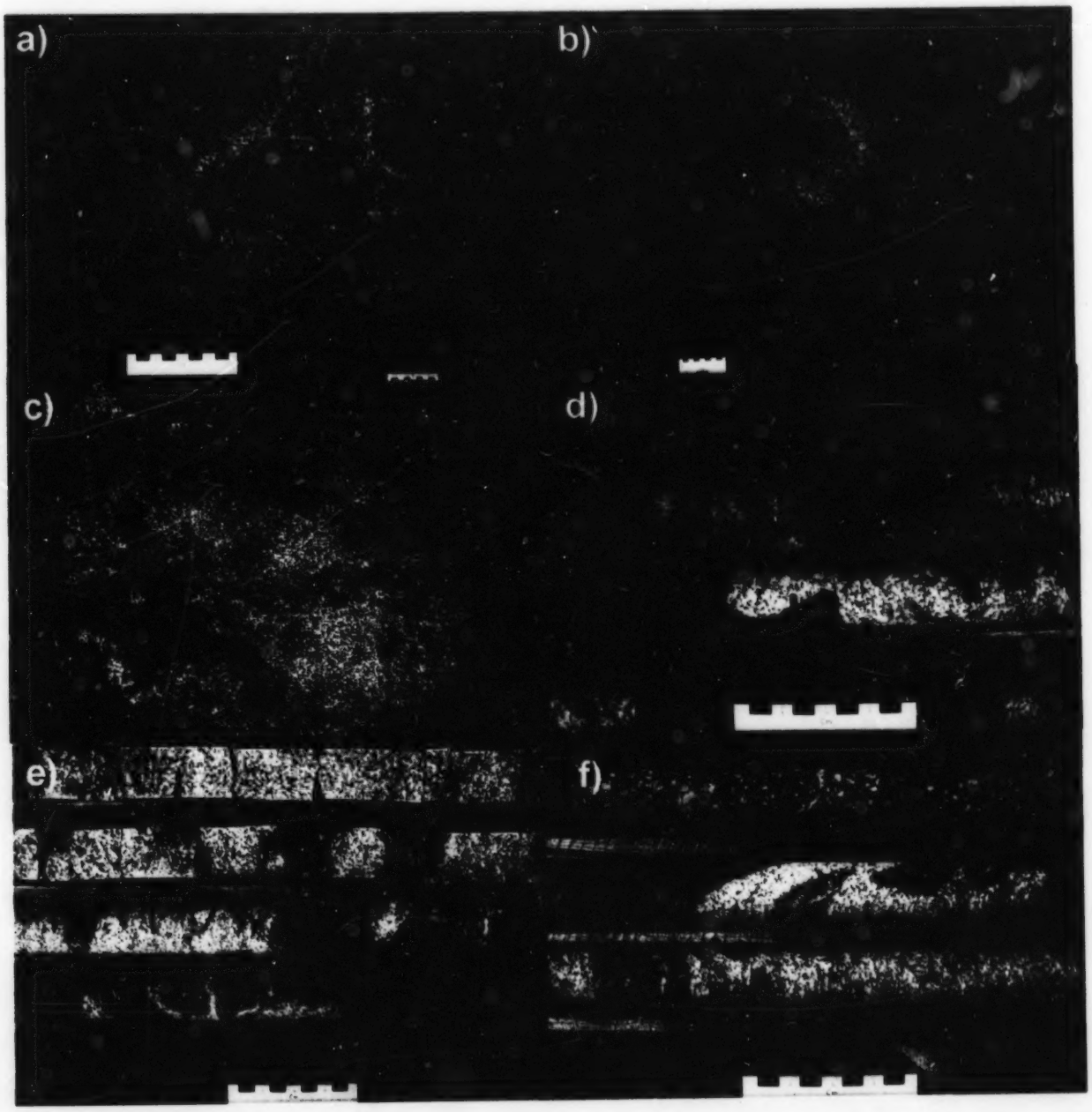

Figure 16: Mixed magma textures in drill core and outcrops in the Ruttan mine area: a) medium-grained tonalite in contact with aphanitic to very fine grained basalt/andesite, Corner Lake pluton, outcrop 2.0 km south of Ruttan pit; note chilled margins at edge of mafic material locally, and back-veining of lower temperature felsic material into quenched basalt; b) medium-grained tonalite/granodiorite in contact with quenched basalt, Corner Lake pluton, same outcrop area as Figure 16a; c) decimetre-scale mafic dyke disaggregated into centimetre-scale mafic enclaves, Corner Lake pluton, same outcrop area as Figure 16a; textures in Figures 16a-c suggest mafic magma injection into a partly crystalline, predominantly felsic magma chamber; d) dyke of basalt and medium-grained tonalite/granodiorite cutting intermediate tuff/volcaniclastic rocks, immediately west of West Anomaly lenses, near contact with Brehaut Lake pluton; e) mafic enclaves and pyritic sulphide inclusions in medium-grained tonalite dyke, near Brehaut Lake pluton contact, 0.5 km west of West Anomaly area; f) mafic enclaves in melanocratic tonalite/diorite, Beahaut Lake pluton, 0.5 km west of West Anomaly area.

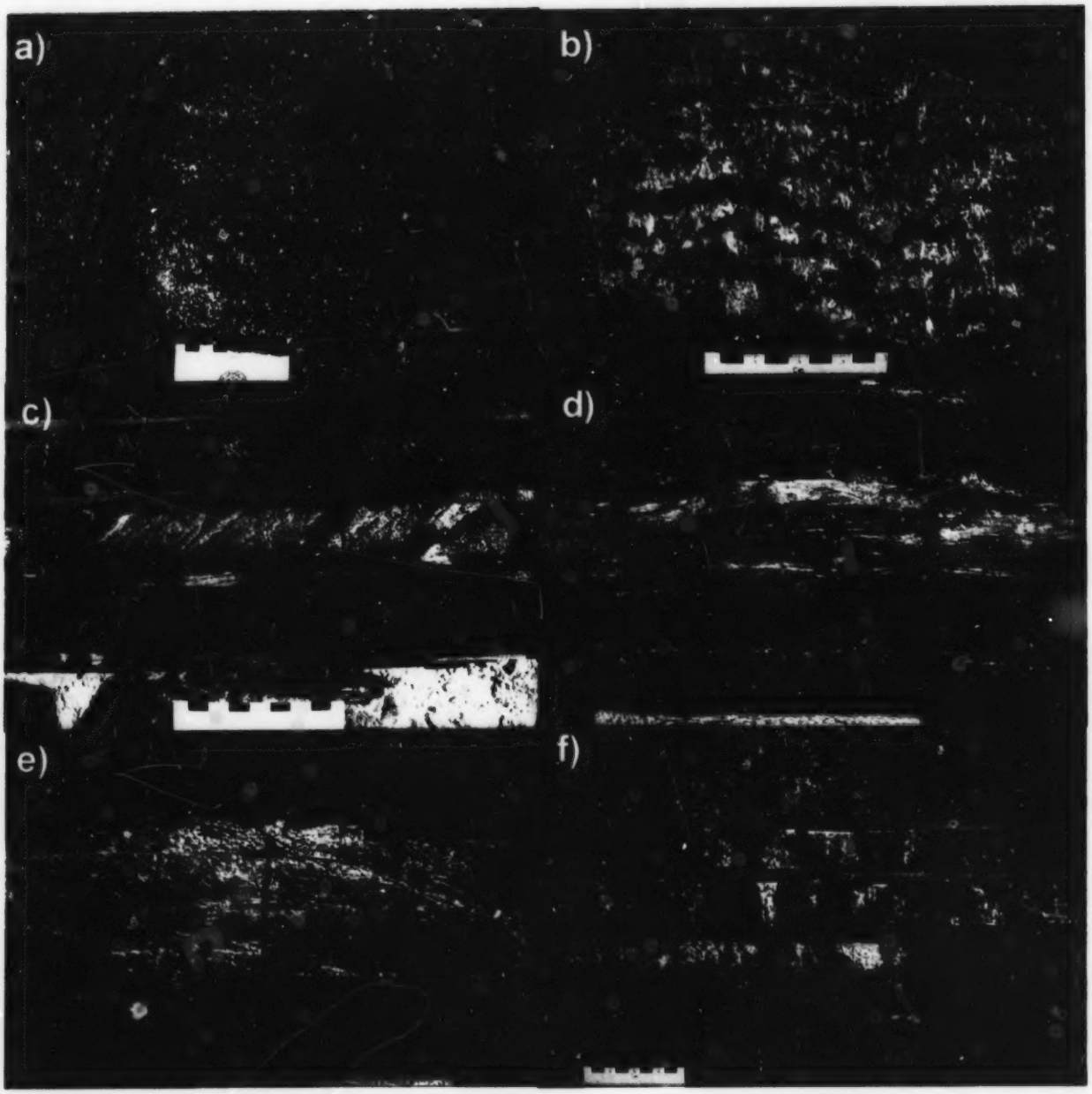

Figure 17: Ore textures in drill core and hand samples from the Ruttan mine area: a) massive Zn ore, with dark brown sphalerite and pyrite as decimetre-scale layers, probably a reflection of primary sedimentation on the paleoseafloor; sample taken undergound from an upper West lenses; b) Zn ore, with centimetre-scale rhythmic layering between light brown sphalerite and pyrite, and white siliceous ash; sample taken from an upper West lenses; c) drill core with massive sulphide, stringer sulphide and garnet-chlorite rock, from footwall contact of lower West lenses; d) siliceous exhalite from 3.1 km along strike to the east-northeast of the centre of the Ruttan pit (location for sample RUT-16); here, this exhalite unit has 1 to 5% sulphide and anomalous Au concentrations (22 ppb); e) network of quartz -filled fractures cutting hanging-wall Powder Magazine Formation volcaniclastic/sedimentary rocks, 0.8 km east-northeast of the eastern edge of the Ruttan pit; f) massive pyritic sulphide intervals along with mafic and intermediate enclaves within Brehaut Lake pluton, 0.5 km west of the West Anomaly area; these sulphide inclusions may represent stoped blocks of the Ruttan orebody.

DISCUSSION

Comparison with Other Large VMS Deposits and their Settings

The Ruttan deposit is clearly a bimodal-siliciclastic type of VMS deposit, similar to those found in the Iberian Pyrite Belt of Portugal and Spain and in the Bathurst district of New Brunswick. In general, bimodal-siliciclastic VMS deposits have approximately equal proportions of volcanic and siliciclastic rocks in the host stratigraphic column (e.g., ±3 km of strata; Barrie and Hannington, 1999). Felsic volcanic rocks are generally more abundant than mafic. The vast majority of bimodal-siliciclastic deposits are Phanerozoic, principally in the Iberian Pyrite Belt and in the Bathurst camp. The felsic host rocks are generally calc-alkalic and, in some cases, it can be argued that they were derived by partial melting of sedimentary sources, consistent with a continental-arc, or rifted continental-arc setting. Mafic rocks are generally tholeiitic, but both the Bathurst district and the Iberian Pyrite belt have mildly alkaline basalt, and arc tholeiite is not uncommon. The bimodal-siliciclastic VMS deposits have the largest average deposit size (23.7 Mt; Barrie and Hannington, 1999). They have, on average, the lowest Cu contents and the highest Pb contents of the five VMS deposit types, which include (Barrie and Hannington, 1999b) bimodal-mafic ('Archean Cu-Zn'), bimodal-felsic ('Kuroko type'), mafic ('ophiolitic') and mafic-siliciclastic ('Besshi type').

It is instructive to compare the geological setting and grade-tonnage data of Ruttan with other VMS deposits. In terms of grade-tonnage data, Ruttan compares closely with Black Mountain, a bimodal-siliciclastic deposit in South Africa; San Nicolas, a bimodal-mafic deposit in Mexico; and TG-1 and TG-3 of the Tambo Grande district in Peru (Table 2). Brief comparisons are made here with other VMS systems, including Black Mountain, Rio Tinto and Neves Corvo in the Iberian Pyrite Belt, and the smaller Fox VMS deposit in the Lynn Lake greenstone belt, approximately 110 km west-northwest of the Ruttan mine. These comparisons suggest that there may be more ore in the immediate vicinity of the Ruttan mine.

Black Mountain, South Africa

In terms of host rock stratigraphy and grade-tonnage data, Ruttan is perhaps most similar to the Black Mountain mine in South Africa. Black Mountain is a bimodal-siliciclastic VMS deposit within the Paleoproterozoic Aggeneys VMS district of northwestern South Africa, near the border with Namibia. It has approximately 82 Mt of 0.75 wt. % Cu, 0.59 wt. % Zn and 2.67 wt. % Pb (Ryan et al., 1986), and is therefore very similar to Ruttan in terms of grade and tonnage. The host rocks are predominantly metasedimentary rocks with subordinate amphibolite (basalt) and leucocratic gneiss (metamorphosed felsic volcanic rocks), in the amphibolite-facies metamorphic grade. At least two other VMS deposits are present within the district (Ryan et al., 1986): Broken Hill (approx. 85 Mt at a similar grade but in a more metasedimentary environment), 5 km along strike; Tank Hill, situated between the two large deposits (no grade-tonnage information); and Big Syncline (approx. 100 Mt at a lower grade, also in a more metased-iment-dominated section). The orebodies in this district are partly linked by magnetite-barite- and locally pyrite-bearing siliceous iron-formation.

Rio Tinto District

Ruttan's stratigraphic setting is very similar to many of the deposits in the Iberian Pyrite Belt of southern Portugal and southeastern Spain. The VMS deposits of the Rio Tinto district (334.5 Mt grading 0.39% Cu, 0.12% Pb, 0.34% Zn, 22 ppm Ag and 0.36 ppm Au; Leistel et al., 1998) occur near the top of a 400 m thick felsic sequence of the Volcano-Sedimentary Formation (VS), in contact with shale and tuffaceous siliciclastic rocks of the overlying Flysch Group (FG). They include the following VMS deposits: San Dionisio in the Corta Atayala open pit, Filon Norte (Solomon), Filon Sur (Lago) and Planes–San Antonio. The VS in the area of the Rio Tinto Anticline comprises mafic volcanic rocks and related hypabyssal sills, felsic volcanic rocks and related hypabyssal sills, and tuffaceous siliciclastic rocks. The deposits occur within an anticlinal axis that extends 8 km from west to east and is itself within a larger syncline. The core of the Rio Tinto anticline contains the Cerro Colorado stockwork deposit, with over 200 Mt of pyritic, low-grade Cu ore. There are other VMS deposits in the immediate vicinity: Chaparrita (0.07 Mt) and Pena de Hierro (5 Mt) are approximately 1.5 km to the north, at the same stratigraphic position as the stratiform Rio Tinto deposits, and the small Masa Valle pyrite deposit lies 0.8 km to the south, slightly up-section in carbonaceous slates and rhyolite ash (Williams et al., 1975). The upper VS contact with the FG is mineralized in numerous locations to the northwest: San Platon (2.5 Mt), San Miguel (1.3 Mt) and the Cueva de la Mora–Casillejito–Aguas Tenidas deposits (>50 Mt), and Conception (56 Mt), which occurs in a panel of VS rocks farther to the north. Regionally, La Zarza (60 Mt) appears to be at the same stratigraphic horizon, approximately 25 km west of Rio Tinto. Sotiel (75 Mt), Valverde (100 Mt) and Tharsis (110 Mt) are within 75 km of Rio Tinto to the south and west within the VS (*see* Barriga and Carvalho, 1997, and references therein). The larger deposits are spaced approximately 15 to 30 km apart from one another and from Rio Tinto, after accounting for approximately 50% Hercynian north-south compression. This is a point worth noting when considering exploration for other large deposits in the RLVB.

Each of the Rio Tinto VMS deposits constitutes a massive, largely pyritic, sulphide blanket underlain by an intense sulphide-chlorite-sericite stockwork. The massive sulphide, which is locally banded, may have formed one continuous blanket over the Cerro Colorado stockwork deposit in the eastern half of the Rio Tinto anticline prior to erosion. Relatively Cu-rich zones are found near the base of the VMS deposits. In many places, the host rock is largely or completely replaced by pyrite, indicating significant subseafloor replacement and a relatively efficient depositional system. The stockwork fractures are present everywhere in the felsic rocks in the core of the anticline, and in many outcrops immediately to the south in the town of Riotinto. Alteration

of footwall rocks is concentric around the intense stringer zones, with an inner intense chloritic zone and a peripheral sericitic zone. The large and well-developed stockwork at Cerro Colorado is in contrast to the footwall rocks at Ruttan, where stockwork and stringer mineralization are limited.

Neves Corvo

The Neves Corvo VMS deposit in the Iberian Pyrite Belt of Portugal also lies within a stratigraphy very similar to that at Ruttan. It has one of the very largest concentrations of sulphide minerals in a VMS system, with more than 300 Mt of sulphide ore (Barriga and Carvalho, 1997). The original resource outlined 42 Mt of Cu-rich ore (7.6% Cu), which also contained 4.3 Mt of material grading 2.5% Sn; an additional 47 Mt had a grade of 6.2% Zn with minor Cu. The geometry of the Neves Corvo deposit is important because it emphasizes that significant ore may be present at distances greater than 1.3 km from Ruttan. At Neves Corvo, the massive sulphide comprises at least five, coalescing, very large, massive-sulphide lenses (maximum dimensions of 0.5–1.0 km for individual lenses) on effectively the same stratigraphic horizon. In total, it extends for more than 2.5 km north to south and 2.0 km east to west. However, there is a 100 to 500 m gap in a central area between the lenses. To one side of this gap is the relatively lean, pyritic Lombador lens, with grades similar to that at Ruttan, and on the other side of the gap are the Neves North and South lenses, which are among the richest in the deposit (Barriga and Carvalho, 1997). This distribution of large, high-grade lenses separated from low-grade lenses by a 100 to 500 m gap provides impetus to explore deeper beneath the low-grade Ruttan lenses.

Fox mine

The Fox Cu-Zn deposit (12 Mt grading 1.82 wt. % Cu and 1.78 wt. % Zn) in the Lynn Lake greenstone belt lies approximately 125 km west-northwest of the Ruttan mine, within a volcanic-volcaniclastic stratigraphic package broadly similar to that at Ruttan. However, there are significant differences:

- a higher volcanic component at Fox that is nearly exclusively mafic
- associated basalt units at Fox that are clearly more magnesian (Gilbert et al., 1982) and occasionally calc-alkalic (Zwanzig et al., 1999)
- a best age estimate of 1910 +15/–10 Ma (Baldwin et al., 1987), approximately 30 m.y. older than the best age estimate for Ruttan

Although the Fox mine is the nearest VMS deposit of significant size to Ruttan, it should not be considered as part of the same VMS district for these reasons.

Controls on Large VMS Deposits: Bulk Crustal Permeability, Crustal-Scale Faults, Magmatic Heat Source

Among the most important controlling factors on the size of a VMS deposit are the permeability of the host-rock stratigraphic succession, and the duration of the magmatic heat source. The presence of a significant siliciclastic component to the host stratigraphic succession favours large VMS deposits, as the largest deposits are either mafic-siliciclastic or bimodal-siliciclastic. This is perhaps not surprising if a continuum with sedimentary-exhalative deposits (SEDEX) is considered. The average SEDEX deposit is 41.3 Mt (n = 62; Lydon, 1996), making it larger than siliciclastic-poor VMS systems by a factor of 8 to 15, but larger than siliciclastic-rich VMS systems by a factor of only 2 to 4 (Barrie et al., 1999). Turbidites are less permeable than volcanic rocks and, in the absence of abundant faulting, a turbidite-rich setting can effectively insulate a hydrothermal cell and its heat source from rapid advective cooling, thus allowing for a longer lived hydrothermal system and relatively efficient, subseafloor metal deposition (Goodfellow et al., 1999).

Fluid Venting Temperatures and Metal Deposition

Vent temperatures can be measured directly on the seafloor, or can be determined by 1) measuring homogenization temperatures in fluid inclusions of vent-fluid precipitates; 2) determining alteration mineral assemblages and considering their stability fields; and 3) considering the solubility of metals in the hydrothermal fluids. Maximum vent temperatures measured for the majority of seafloor sites in mid-ocean ridge, back-arc basin and back-arc spreading centres range from 220 to 380°C; primary fluid-inclusion homogenization temperatures for the majority of VMS deposits studied range from 200 to 350°C (de Ronde, 1995). Higher salinity fluids can have higher vent temperatures (e.g., up to approx. 420°C at approx. 15–20 wt. % NaCl in the Atlantis II Deeps of the Red Sea; Ramboz et al., 1988) and have the ability to transport greater concentrations of metals. The stability of alteration mineral assemblages in vent areas can provide a reliable estimate of the average vent temperatures (Alt, 1999). The sulphide mineral assemblage in VMS deposits is dependent, in part, on fluid temperature and can be used to estimate vent or paleovent temperatures. This can be accomplished by comparison with direct measurements of minerals precipitating from venting hydrothermal fluids on the seafloor (Hannington et al., 1995), or by consideration of the temperature dependence of metal solubility in hydrothermal solutions. Temperature ranges are estimated assuming that chalcopyrite, sphalerite and galena will precipitate from fluids saturated at Cu, Zn and Pb contents, respectively, of 1 to 100 ppm (Large, 1992).

The ability of a hydrothermal fluid to transport and deposit metals is related to fluid temperatures; to intrinsic parameters that

include the pH, salinity, H_2S and fO_2 of the fluid and that themselves are dependent on interaction with host rocks and sulphide; and possibly to pressure (Seyfried et al., 1999). The stability and kinetics of metal mineral species are also important. Regarding metal solubilities in hydrothermal fluids, it is common practice to consider approximately 100 ppm of Cu+Zn+Pb in a hydrothermal fluid available for precipitation (Cathles, 1983). These values are higher by an order of magnitude than the measured values in the majority of vent fluids, which are commonly undersaturated, because it is proper to consider the metal content of the rising hydrothermal fluid *prior to metal deposition* in the subseafloor environment. A review of the experimental and theoretical controls on the composition of mid-ocean ridge hydrothermal fluids is provided in Seyfried et al. (1999).

The efficiency of metal deposition at or beneath the seafloor is an important constraint on the heat and fluid flow of a VMS system. If the depositional efficiency is very low, then it is necessary for more hydrothermal fluid to vent in order to precipitate a given tonnage of ore. This can be accomplished by a higher venting rate or a longer duration, or both. Individual vent sites have vent rates ranging from tens of cm^3/s to m^3/s, and may be active for periods of days to hundreds of years (Hannington et al., 1995). Converse et al. (1984) calculated a low depositional efficiency of less than 3% for sulphide-particle settling from a hydrothermal plume along the East Pacific Rise. Applying Stokes law to settling velocities for fine sulphide particulate matter in vent plumes, Cathles (1983) calculated that unusually quiescent conditions are necessary for sulphide to accumulate by this process. There are no examples of VMS deposits that are believed to have formed exclusively by sulphide-particle settling, suggesting that depositional efficiency must be greater than 3%. At the other end of the spectrum, depositional efficiency approaches 100% in quiescent brine pools in the Red Sea (Zierenberg, 1992), and is considered very high in other VMS environments that have thick, fine-grained siliciclastic sediment (e.g., parts of Middle Valley along the northern Juan de Fuca Ridge; Goodfellow et al., 1999). The presence of stockwork stringer zones and sulphide replacement textures in many VMS deposits indicates subseafloor deposition. Local diffuser structures, such as the 'beehive structure' of the Snakepit hydrothermal field (Mid-Atlantic Ridge, latitude 23°N), cool the venting hydrothermal fluids from 345 to 70°C and are highly efficient at sequestering metals from the fluid (Fouquet et al., 1993). Detailed heat- and fluid-flow analysis of specific active seafloor hydrothermal systems may eventually allow for accurate estimations of the depositional efficiency in paleohydrothermal systems.

Heuristic Calculations: Volume of Hydrothermal Fluid Necessary to Form the Ruttan VMS Deposit

It is instructive to estimate the volume of hydrothermal fluid necessary to form the Ruttan deposit, and then to estimate the minimum size of intrusion necessary to heat hydrothermal fluids sufficiently to leach and precipitate the base metals. Such calculations are particularly useful when setting up heat- and fluid-flow models to consider how the deposit formed. Ruttan has approximately 2.5 Mt of contained Cu+Zn. Although there have been no fluid-inclusion studies, the generally low tenor of Cu+Zn and the abundance of pyrite can be interpreted to reflect venting at relatively low temperatures. For this calculation, we take approximately 250°C as an average venting temperature to form the deposit, recognizing that fluids from 200 to 300°C must have been present in the vent area. This average temperature is lower than most modern seafloor black-smoker hydrothermal systems by approximately 50°C (Hannington et al., 1995). We note that this temperature estimate is provisional, as there is some basis for considering higher temperatures, with some of the base metals leached (or zone refined) out of the system; resolution of this debate must await fluid-inclusion studies. The amount of metal a hydrothermal fluid can transport depends on temperature. In typical seafloor hydrothermal fluids, Zn solubility increases from 1 to 100 ppm as temperature increases from 175 to 240°C, and Cu solubility increases from 1 to 100 ppm as temperature increases from 260 to 360°C (Large, 1993). For this example, we take an average of 20 ppm Cu+Zn in the average hydrothermal fluid. This corresponds to 1.25×10^{11} t of hydrothermal fluid at 250°C being required to transport 2.5 Mt of Cu+Zn.

As outlined in Barrie et al. (1999), the relationship between the maximum mass of hydrothermal fluid venting at 250°C and the heat of the source intrusion can be estimated:

(magma temperature – 250°C) x (mass of intrusion) x (1/3 cal/g°C) = (250°C – 0°C) x (mass of hydrothermal fluid) x (1 cal/g°C)

An estimate of 800°C for the temperature of a hypothetical magma chamber at depth, perhaps at considerable depth, that is known to be active at the time of ore formation comes from the zircon geothermometry for the Mine Sequence rhyolite (described previously). Using the above equation, a 63 km^3 felsic intrusion is the minimum size required to drive the hydrothermal fluids necessary to transport the Cu and Zn at Ruttan; this translates into a 1 km thick felsic sill with a 9 km diameter.

Role of Anhydrite in VMS Systems

The presence of anhydrite at Ruttan and near two of the Darrol Lake deposits is interesting, both empirically and from a genetic point of view. From the initial results of this reconnaissance study, the presence of anhydrite appears to reflect proximity only to significant accumulations of base-metal–bearing massive sulphide. Anhydrite precipitates from seawater at approximately 100 to 150°C as temperature increases; conversely, it dissolves down-temperature from 150 to 0°C. Examples of anhydrite precipitation near and within seawater-related hydrothermal systems come from Iceland and at mid-ocean ridges. In the Reykjanes geothermal systems of Iceland, an impermeable seal forms around the venting area on a scale of hundreds of metres as the host basalt is plugged, principally by anhydrite (Tomasson and Kristmansdottir, 1972). Seawater outside the anhydrite seal is at 12°C to a depth of 200 m, whereas the hydrothermal fluids inside the seal are at 150°C at a depth of 200 m. At Reykanes, the hydrothermal fluids are generally modified meteoric water, but there are invasions of seawater into the venting area during tectonic disturbances.

Anhydrite precipitation is documented in Ocean Drilling Program (ODP) hole 504B, and also in the TAG hydrothermal deposits (e.g., Alt et al., 1989; Mills et al., 1998; Teagle et al., 1997). At TAG, much of the anhydrite formed as breccia cement in the stockwork zone under the deposit, but has since dissolved due to an influx of cooler seawater during the waning stages of the hydrothermal system. Anhydrite has retreated to higher temperature areas, either at greater depths in the plumbing system, or near the vent areas.

Approximately 0.14 mass percent of anhydrite can precipitate from pristine seawater, and up to 0.38 mass percent can precipitate if Ca is leached from basalt (Moller, 1988). Sleep (1991) incorporated anhydrite solubility into a two-dimensional heat- and fluid-flow model of a mid-ocean ridge, and determined that approximately 0.7 volume and mass percent anhydrite could precipitate, which would clog fractures and occlude permeability to a significant degree in the sheeted dyke complex. Anhydrite must precipitate to a significant degree in any seawater-related hydrothermal system that has temperatures of 150°C or greater, and must therefore affect permeability and the geometry of the hydrothermal system. Unpublished calculations of the temperature and pressure dependence indicate that, under ideal circumstances, anhydrite plugging can decrease bulk permeability by two to three orders of magnitude.

Unfortunately, anhydrite is uncommon in ancient VMS deposits as it generally dissolves in the presence of lower temperature fluids, and selvaging by massive anhydrite precipitation has never been clearly documented in either modern or ancient systems. It is possible that the anhydrite at Ruttan could reflect the hydrothermal system that formed the deposit, possibly the waning stages of the hydrothermal system, as seen at TAG. There are two other possibilities:

- The anhydrite may have been produced during upper greenschist to amphibolite facies metamorphism at Ruttan and in the southern Rusty Lake volcanic belt generally. During metamorphism, sulphide minerals may react with oxidizing fluids and/or react with calcic phases under relatively oxidizing conditions to produce minor anhydrite (e.g., Geco, several Flin Flon deposits, several deposits in Scandanavian Caledonides; Cook and Hoefs, 1997).
- The anhydrite may be due to a reaction of the massive sulphide with oxidized connate waters at relatively high temperatures, possibly during burial in the Paleozoic.

However, these options do not explain the apparent preferred association of the anhydrite in the hanging wall at Ruttan. These possibilities could be examined by a sulphur-isotope study on the anhydrite and sulphide phases.

Post-VMS Low-Temperature Venting: Regional Exhalite–Iron-Formation

The regional exhalite and iron-formations in the RLVB may be both directly and indirectly related to the hydrothermal system that formed the Ruttan orebody. Regional exhalite–iron-formation units are common in VMS districts, and they have a variety of features (Spry et al., 2000). For example, chert is abundant in the Iberian Pyrite Belt and is typically found in two horizons in the Volcano-Sedimentary formation (VS): a lower horizon, equivalent to the purple shale marker horizon, and an upper chert horizon or horizons that may contain manganese deposits, clearly up-section from VMS mineralization (Strauss et al., 1981). Neither horizon is found directly along strike from VMS deposits (Leistel et al., 1998). The chert is attributed to low-temperature hydrothermal venting on the paleoseafloor. Barriga and Fyfe (1988) suggested that the chert was a seafloor precipitate that insulated the subsurface and formed an impermeable cap to the VS, which would have caused focusing of upwelling hydrothermal fluids, both of which would favour VMS formation. The Pb isotopic signature of the upper chert horizons is always more radiogenic than VMS deposits, indicating a separate source for the lead and the hydrothermal fluids, probably influenced by younger sediments and seawater (Leistel et al., 1998). Recent heat- and fluid-flow modelling of the Rio Tinto system (Barrie et al., work in progress) suggests that hanging-wall chert may be a consequence of the waning stages of this very large hydrothermal system, a system that continued at low temperatures in the upper crust for tens to hundreds of thousands of years after ore deposition, in the absence of significant tectonic disturbance. This scenario may also be applicable to regional exhalites and iron-formations in the Ruttan region.

Spacing of Crustal-Scale Hydrothermal Systems

In some VMS districts, there is a regular spacing of VMS deposits along preferred horizons. At Mattagami, for example, many of the 1 to 5 Mt deposits are present at a 3 to 5 km spacing along the Key Tuffite horizon. This may be attributable to a relatively shallow, subhorizontal heat source intrusion in the underlying Bell River Gabbroic Complex. Regularly spaced hydrothermal upwelling is predicted mathematically for fluids in a porous medium heated uniformly from below (Lapwood, 1948). Perhaps a more appropriate setting for comparisons to Ruttan is found in the eastern Iberian Pyrite Belt, where the larger deposits or districts (greater 40 Mt) are regularly spaced at approximately 15 to 30 km. If these formed synchronously, this would suggest that a very large and deep heat source was responsible for the hydrothermal systems, possibly ponded mafic and felsic magmas in the middle crust below the brittle-ductile transition, at a depth of 10 to 20 km. It is interesting to note that similar spacings for hydrothermal cells are observed in active rift-related settings such as the Salton Sea area of southern California and the Taupo volcanic zone and geothermal area of New Zealand.

There is indirect evidence, from the Pb isotopic signatures of VMS deposits across the Iberian Pyrite Belt, to support deeply penetrating hydrothermal fluids. Marcoux (1998) found that the Pb isotopic signatures of most Iberian Pyrite Belt VMS deposits

are relatively uniform, and have an Early Paleozoic to Late Proterozoic signature distinct from the upper Phyllite-Quartzite Group (PQ) and consistent with newly analyzed xenocrystic zircon in Volcano-Sedimentary Formation (VS) rhyolite (Barrie et al., work in progress). Similar zircon inheritance would be expected for U-Pb geochronology studies in the Rusty Lake volcanic belt. For the Iberian Pyrite Belt, Marcoux (1998) envisioned crustal-scale, coeval hydrothermal systems driven by 'magmatic-floor heating', rather than isolated systems that would be more likely to have more provincial isotopic signatures. Deeply penetrating hydrothermal fluids were also envisioned by Mills et al. (1987) for the Navan Pb-Zn deposits in Ireland, based on Pb isotope signatures.

CONCLUSIONS AND RECOMMENDATIONS FOR FURTHER WORK

New observations have been made for the sedimentary and volcanic rocks near the Ruttan mine and the Darrol Lake deposits in the southern Rusty Lake volcanic belt (RLVB). The hanging-wall Power Magazine Formation includes at least one polyfragmental agglomerate unit, more than 50 m thick, that contains mafic bombs and scoriaceous felsic fragments, proximal to the Ruttan mine. This unit may extend to the north and east for several kilometres, and overlie fine-grained siliciclastic rocks above the orebody. It may represent a lahar derived from a paleotopographic high to the east. The presence of mafic and felsic juvenile fragments in the agglomerate of Powder Magazine Formation, and felsic dykes that branch out as sills along paleohorizontal partings in the volcanic and volcaniclastic units up-section from the mine, suggest that bimodal volcanism and at least felsic magmatism were active shortly after formation of the Ruttan orebody.

Initial results from an X-ray diffractometry study of the alteration mineralogy show that the most diagnostic minerals proximal to significant base-metal mineralization are cordierite, carbonate minerals and anhydrite. Anhydrite is particularly interesting, as it is uncommon in pre-Paleozoic VMS deposits and is an indicator of the paleohydrothermal system that formed the deposit. Initial results from a study of the metal and trace-element contents of exhalites at Ruttan and Darrol Lake indicate that positive Eu anomalies are present proximal to significant ore, whereas negative Eu anomalies are present elsewhere. Positive Eu anomalies reflect high-temperature paleoseafloor hydrothermal vent fluids that have the ability to leach and transport significant quantities of base metals, and they are therefore an excellent indicator of proximity to significant base-metal deposits in the southern Rusty Lake volcanic belt.

A comparison of Ruttan to other large VMS deposits around the world indicates that this deposit is most similar geologically and in terms of metal contents to Black Mountain in the Aggeneys district of South Africa. Black Mountain is 1) a bimodal-siliciclastic VMS deposit, 2) Paleoproterozoic in age, 3) approximately 82 Mt in size, and 4) 0.75 wt. % Cu, 0.59 wt. % Zn and 2.67 wt. % Pb (Ryan et al., 1986). The Black Mountain deposit is within a district that includes at least two other smaller VMS deposits, Broken Hill and Big Syncline. Additionally, comparisons can be made with other very large VMS systems in the Iberian Pyrite Belt, including Neves Corvo and Rio Tinto. These comparisons suggest that there may be more ore in the immediate vicinity of the Ruttan mine.

Recommendations

1) All public-domain and company geological and geochemical data for the RLVB needs to be compiled, and a new lithological map at 1:100 000 scale generated, with an emphasis on mineral deposit potential.
2) Following the success of this pilot study, the metal and trace-element geochemistry of iron-formations and exhalite horizons in the entire RLVB needs to be analyzed and interpreted comprehensively to locate new significant base-metal targets.
3) The potential for additional Cu-Zn resources down-plunge from the Ruttan ore lenses at depths of greater than 1.3 km needs to be considered carefully before mine closure. There is precedent for the discovery of base-metal–rich massive-sulphide lenses along the same horizon as lower grade lenses in bimodal-siliciclastic VMS systems (e.g., Neves Corvo, Portugal).
4) The relative timing of volcanism, intrusive activity, sedimentation and deformation in the RLVB is essentially unconstrained. Both conventional and sensitive high-resolution ion microprobe (SHRIMP) U-Pb geochronological studies are necessary to help build the volcanic and sedimentary stratigraphy and deformation history.
5) More information is needed to determine the potential spacing of large VMS deposits in the RLVB, including a) the extent of the geochemical, mineralogical (including XRD studies, with an emphasis on anhydrite) and oxygen and sulphur isotopic signatures of the alteration halo in the hanging wall at Ruttan; b) estimates of the temperature of venting at Ruttan from fluid inclusions in the gangue of the massive sulphide; and c) the Pb isotopic signatures of the mines and occurrences, which may help determine how deeply the hydrothermal systems penetrated into the crust.
6) Once these aspects are in place, GIS-based mineral-potential mapping should be undertaken to prioritize base-metal target areas in the RLVB.
7) A comprehensive geological, geochemical, mineralogical and geophysical investigation of the Ruttan Cu-Zn deposit should be undertaken and published before mine closure. This would benefit future exploration in the region and economic geologists around the world.

ACKNOWLEDGMENTS

Reg Yarowski of Hudson Bay Mining and Smelting Co. Ltd. (HBMS) at the Ruttan mine, Kelly Gilmore of HBMS in Flin Flon, David Corrigan of the Geological Survey of Canada, and Chris Beaumont-Smith and Ric Syme of the Manitoba Geological Survey have all been helpful with logistical support and geological insights for this project. Jamil Sader and Andy Roberts are thanked for help with X-ray diffractometry, and Stephanie Douma and Christina Taylor are thanked for help with drafting. Jan Peter and Mark Hannington at the Geological Survey of Canada are thanked, the former for discussions and reprints regarding VMS-related exhalites and iron-formations, and the latter for discussions regarding modern seafloor hydrothermal systems, and metamorphic anhydrite. Bob Davie of RnD Technical edited this report on short notice and did an exemplary job. Paul Lenton of Manitoba Industry, Trade and Mines formatted the figures, and kindly provided digital information in support of this project. This study is part of a Targeted Geoscience Initiative project entitled 'Tectonostratigraphic Setting and Mineral Potential of Volcano-Sedimentary Belts along the Granville Lake–South Indian Lake Transect, Northern Manitoba', David Corrigan, Project Co-ordinator.

REFERENCES

Alt, J.C. 1999: Hydrothermal alteration and mineralization of oceanic crust: mineralogy, geochemistry and processes; *in* Volcanic-Associated Massive Sulfide Deposits: Processes and Examples in Modern and Ancient Settings, (ed.) C.T. Barrie and M.D. Hannington; Reviews in Economic Geology, v. 8, p. 133–156.

Alt, J.C., Anderson, T.F. and Bonnell, L. 1989: The geochemistry of sulfur in a 1.3 km section of hydrothermally altered oceanic crust, DSDP hole 504B; Geochimica et Cosmochimica Acta, v. 53, p. 1011–1023.

Ames, D.E. 1996: Stratigraphic and tectonic setting of the Paleoproterozoic Ruttan Cu-Zn VHMS deposit, Rusty Lake belt, Trans-Hudson Orogen; *in* EXTECH 1: A Multidisciplinary Approach to Massive Sulphide Research in the Rusty Lake–Snow Lake Greenstone Belts, Manitoba, (ed.) G.F. Bonham-Carter, A.G. Galley and G.E.M. Hall; Geological Survey of Canada, Bulletin 426, p. 15–43.

Ames, D.E. and Taylor, C. 1996: Geology of the West Anomaly orebody, Ruttan volcanic-hosted massive sulphide deposit, Proterozoic Rusty Lake belt; *in* EXTECH 1: A Multidisciplinary Approach to Massive Sulphide Research in the Rusty Lake–Snow Lake Greenstone Belts, Manitoba, (ed.) G.F. Bonham-Carter, A.G. Galley and G.E.M. Hall; Geological Survey of Canada, Bulletin 426, p. 45–76.

Bailes, A.H. and Galley, A.G. 1996: Setting of Paleoproterozoic volcanic-hosted massive base metal sulphide deposits, Snow Lake; *in* EXTECH 1: A Multidisciplinary Approach to Massive Sulphide Research in the Rusty Lake–Snow Lake Greenstone Belts, Manitoba, (ed.) G.F. Bonham-Carter, A.G. Galley and G.E.M. Hall; Geological Survey of Canada, Bulletin 426, p. 105–138.

Baldwin, D.A. 1980: Ruttan Lake, Karsakuwigamak Lake, Eagle Lake project; *in* Report of Field Activities 1980, Manitoba Energy and Mines, Mineral Resources Division, p. 14–18.

Baldwin, D.A. 1988: Geology of the southern part of the Rusty Lake volcanic belt; Manitoba Energy and Mines, Geological Services, Geological Report 86-1, 90 p.

Baldwin, D.A., Syme, E.C., Zwanzig, H.V., Jordon, T.M., Hunt, P.A. and Stevens, R.D. 1987: U-Pb zircon ages from the Lynn Lake and Rusty Lake metavolcanic belts, Manitoba: two ages of Proterozoic magmatism; Canadian Journal of Earth Sciences, v. 24, p. 1053–1063.

Barrie, C.T. 1995: Zircon thermometry of high-temperature rhyolites near volcanic-associated massive sulfide deposits, Abitibi Subprovince, Canada; Geology, v. 23, p. 169–172.

Barrie, C.T. and Hannington, M.D. 1999: Classification of volcanic-associated massive sulfide deposits based on host-rock composition; *in* Volcanic-Associated Massive Sulfide Deposits: Processes and Examples in Modern and Ancient Settings, (ed.) C.T. Barrie and M.D. Hannington; Reviews in Economic Geology, v. 8, p. 1–12.

Barrie, C.T., Cathles, L.M., Erendi, A., Schwaiger, H., and Murray, C. 1999: Heat and fluid flow models and VMS systems; *in* Volcanic-Associated Massive Sulfide Deposits: Processes and Examples in Modern and Ancient Settings, (ed.) C.T. Barrie and M.D. Hannington; Reviews in Economic Geology, v. 8, p. 201–220.

Barrie, C. T., Zagorevski, A., Lydon, J. W., Jenkins, C. L., Hannington, M. D., Franklin, J. M. and Hillary, E. in press: Volcanogenic massive sulfide deposits of the world; Geological Survey of Canada, Open File Report, index level database and CD-ROM.

Barriga, F.J.A.S. and Carvalho, D. 1997: Geology and VMS deposits of the Iberian Pyrite Belt; Society of Economic Geologists, Guidebook Series, v. 27, 192 p.

Barriga, F.J.A.S. and Fyfe, W.S. 1988: Giant pyritic base-metal deposits: the example of Feitais (Aljustrel, Portugal); Chemical Geology, v. 69, p. 331–343.

Cathles, L.M. 1983: An analysis of the hydrothermal system responsible for massive sulfide deposition in the Hokuroku basin of Japan; *in* The Kuroko and Related Volcanogenic Massive Sulfide Deposits; Economic Geology Publishing Co., Lancaster, Pa., Economic Geology Monograph 5, p. 439–487.

Cook, N.J. and Hoefs, J. 1997: Sulphur isotope characteristics of metamorphosed Cu-(Zn) volcanogenic massive sulphide deposits in the Norwegian Caledonides; Chemical Geology, v. 135, p. 307-324.

Converse, D.R., Holland, H.D. and Edmond, J.M. 1984: Flow rates in the axial hot springs of the East Pacific Rise (21°N): implications for the heat budget and the formation of massive sulfide deposits; Earth and Planetary Science Letters, v. 69, p. 159–175.

de Ronde, C.E.J. 1995: Fluid chemistry and isotopic characteristics of seafloor hydrothermal systems and associated VMS deposits: potential for magmatic contributions; *in* Magmas, Fluids and Ore Deposits, (ed.) J.F. Thompson; Mineralogical Association of Canada, Short Course Series, v. 23, p. 479–510.

Fouquet, Y., Wafik, A., Cambon, P., Nevel, C., Meyer, G. and Gente, P. 1993: Tectonic setting and mineralogical and geochemical zonation in the Snakepit sulfide deposit (Mid-Atlantic Ridge at 23°N); Economic Geology, v. 88, p. 2018–2036.

Gilbert, P., Zwanzig, H.V., Chornoby, P.J. and Olson, P.E. 1982: Stratigraphy of the Lynn Lake greenstone belt and surface geology at Ruttan and Fox mine; Geological Association of Canada, Field Trip Guidebook, Winnipeg, 59 p.

Goodfellow, W.D., Zierenberg, R. A. and ODP Leg 169 Shipboard Science Party 1999: Genesis of massive sulfide deposits at sediment-covered spreading centers; *in* Volcanic-Associated Massive Sulfide Deposits: Processes and Examples in Modern and Ancient Settings, (ed.) C.T. Barrie and M.D. Hannington; Reviews in Economic Geology, v. 8, p. 297–324.

Hannington, M.D., Barrie, C.T. and Bleeker, W. 1999: The Giant Kidd Creek volcanogenic massive sulfide deposit, Western Abitibi Subprovince, Canada; *in* The Giant Kidd Creek Volcanogenic Massive Sulfide Deposit, Western Abitibi Subprovince, Canada, (ed.) M.D. Hannington and C.T. Barrie; Economic Geology Publishing Co., Lancaster, Pa., Economic Geology Monograph 8, p. 1–30.

Hannington, M.D., Jonasson, I.R., Herzig, P.M. and Petersen, S. 1995: Physical and chemical processes of seafloor mineralization at mid-ocean ridges; *in* Seafloor Hydrothermal Systems: Physical, Chemical, Biological and Geological Interactions, (ed.) S.E. Humphris, R.A. Zierenberg, L.S. Mullineaux and R.E. Thomson; American Geophysical Union, Washington, D.C., Geophysical Monograph 91, p. 115–157.

Lapwood, E.R. 1948: Convection of a fluid in a porous medium; Cambridge Philosophical Society Proceedings, v. 44, p. 508–521.

Large, R.R. 1992: Australian volcanic-hosted massive sulfide deposits: features, styles and genetic models; Economic Geology, v. 87, p. 471–510.

Leistel, J.M., Marcoux, E., Thieblemont, D., Quesada, C., Sanchez, A., Almodovar, G.R., Pascual, E. and Saez, R. 1998: The volcanic-hosted massive sulphide deposits of the Iberian Pyrite Belt; Mineralium Deposita, v. 33, p. 2–30.

Lesher, C.M., Goodwin, A.M., Campbell, I.H. and Gorton, M. P. 1986: Trace-element geochemistry of ore-associated and barren, felsic metavolcanic rocks in the Superior Province, Canada; Canadian Journal of Earth Sciences, v. 23, p. 222–237.

Lottermoser, B.G. 1989: Rare earth element study of exhalites within the Willyama Supergroup, Broken Hill block, Australia; Mineralium Deposita, v. 24, p. 92–99.

Luff, W.M., Goodfellow, W.D. and Juras, S.J. 1992: Evidence for feeder pipe and associated alteration at Brunswick #12 massive sulfide deposit; Exploration and Mining Geology, v. 1, p. 167–185.

Lydon, J.W. 1996: Sedimentary exhalative sulphides (SEDEX); *in* Geology of Canadian Mineral Deposit Types, (ed.) O.R. Eckstrand, W.D. Sinclair and R.I. Thorpe; Geological Survey of Canada, Geology of Canada, no. 8, p. 130–152.

Marcoux, E. 1998: Lead isotope evidence of the giant massive sulphide deposits in the Iberian Pyrite Belt; Mineralium Deposita, v. 33, p. 45–58.

Michard, A. 1989: Rare earth element systematics in hydrothermal fluids; Geochemica et Cosmochimica Acta, v. 53, p. 745–750.

Mills, H., Halliday, A.N., Ashton, J.H., Anderson, I.K. and Russell, M.J. 1987: Origin of a giant orebody at Navan, Ireland; Nature, v. 327, p. 223–226.

Mills, R.A., Teagle, D.A.H. and Tivey, M.K. 1998: Fluid mixing and anhydrite precipitation within the TAG mound; Proceedings of the Ocean Drilling Program, Scientific Results, v. 158, p. 119–127.

Moller, N. 1988: The prediction of mineral solubilities in natural waters: a chemical equilibrium model for the Na-Ca-Cl-SO_4-H_2O system, to high temperature and concentration; Geochimica et Cosmochimica Acta, v. 52, p. 821–837.

Peter, J.M. and Goodfellow, W. D. in press: Hydrothermal sedimentary rocks of the Heath Steele belt, Bathurst Mining camp, New Brunswick: 3. Application of mineralogy, mineral and bulk compositions to massive sulfide exploration; Geological Association of Canada, Special Volume (on the Bathurst VMS district).

Ramboz, C., Oudin, E. and Thisse, Y. 1988: Geyser-type discharge in Atlantis II deep, Red Sea: evidence of boiling from fluid inclusions in epigenetic anhydrite; Canadian Mineralogist, v. 26, p. 765–786.

Ryan, P.J., Lawrence, A.L., Lipson, R.D., Moore, J.M., Paterson, A., Stedman, D.P. and Van Zyl, D. 1986: The Aggeneys base metal sulphide deposits, Namaqualand District; *in* Mineral Deposits of South Africa, (ed.) C.R. Anhaeusser and S. Maske; Geological Society of South Africa, v. 1, p. 1447–1473.

Seyfried, W.E., Jr., Ding, K., Berndt, M.E. and Chen, X. 1999: Experimental and theoretical controls on the composition of mid-ocean ridge hydrothermal fluids; *in* Volcanic-Associated Massive Sulfide Deposits: Processes and Examples in Modern and Ancient Settings, (ed.) C.T. Barrie and M.D. Hannington; Reviews in Economic Geology, v. 8, p. 181–200.

Sleep, N.H. 1991: Hydrothermal circulation, anhydrite precipitation and thermal structure at ridge axes; Journal of Geophysical Research, v. 96, p. 2375–2387.

Speakman, D.S., Chornoby, P.J., Holmes, G.F. and Haystead, B.C.W. 1982: Geology of the Ruttan deposit; Geological Association of Canada, Special Paper 25, p. 525–555.

Spry, P.G., Peter, J.M. and Slack, J. F. 2000: Meta-exhalites as exploration guides to ore; *in* Reviews in Economic Geology, v. 11, p. 163–201.

Stern, R.A., Syme, E.C., Bailes, A.H. and Lucas, S.B. 1995: Paleoproterozoic (1.90–1.86 Ga) arc volcanism in the Flin Flon belt, Trans-Hudson Orogen, Canada; Contributions to Mineralogy and Petrology, v. 119, p. 117–141.

Strauss, G.K., Roger, G., Lecolle, M. and Lopera, E. 1981: Geochemical and geologic study of the volcano-sedimentary sulfide orebody of La Zarza, Huelva Province; Economic Geology, v. 76, p. 1975–2000.

Teagle, D.A.H., Alt, J.C., Chiba, S., Humphris, S. and Halliday, A.N. 1997: Strontium and oxygen isotopic constraints on fluid mixing, alteration and mineralization in the TAG hydrothermal deposit; Chemical Geology, v. 149, p. 1–24.

Tomasson, J. and Kristmannsdottir, J. 1972: High temperature alteration minerals and thermal brines, Reykjanes, Iceland; Contributions to Mineralogy and Petrology, v. 36, p. 123–134.

Watson, E.B. and Harrison, T.M. 1983: Zircon saturation revisited: temperature and composition effects in a variety of crustal types; Earth and Planetary Science Letters, v. 64, p. 295–304.

Williams, D., Stanton, R.L. and Rambaud, F. 1975: The Planes–San Antonio pyritic deposit of Rio Tinto, Spain: its nature, environment and genesis; Transactions of the Institute of Mining and Metallurgy, London, v. B84, p. 73–82.

Zierenberg, R.A. 1990: Deposition of metalliferous sediment beneath a brine pool in the Atlantis II Deep, Red Sea; *in* Gorda Ridge: A Seafloor Spreading Center in the United States Exclusive Economic Zone, (ed.) G.R. McMurry; Springer-Verlag, New York, p. 131–142.

Zwanzig, H.V., Syme, E.C. and Gilbert, H.P. 1999: Updated trace element geochemistry of ca. 1.9 Ga metavolcanic rocks in the Paleoproterozoic Lynn Lake Belt; Manitoba Industry, Trade and Mines, Geological Services, Open File Report OF99-13, 46 p.

APPENDIX A – X-RAY DIFFRACTION AND JADE™ PATTERN-PROCESSING METHODOLOGY

X-Ray Diffraction Methodology

The mineralogy of powdered whole-rock samples can be determined by X-ray powder diffraction analysis (XRD). Each powdered sample is first tested for magnetism with a magnet and tested for $CaCO_3$ using weak (10%) HCl. The powder is then placed in circular powder mounts that have a hollow void in the centre and compressed by hand. The top is smoothed so that it is flush. The prepared samples are then measured for their X-ray patterns using the Philips PW1710 automated powder diffractometer equipped with a graphite monochromator and using Co K alpha radiation at 40kV and 30mA, at a rate of 0.1 degrees per second, from 2 degrees to 74 degrees (2θ).

JADE™ 3.1 Pattern Processing

JADE™ 3.1 Pattern Processing (Materials Data, Inc.) is a PC-based program that assists in the analysis of X-ray powder-diffraction patterns in terms of the mineralogical mode. The X-ray patterns can be rescaled and shifted to identify minerals in each sample to semiquantitative accuracy. The Powder Diffraction File (PDF) of the International Centre for Diffraction Data (ICDD) database is used with JADE analysis of XRD patterns. A reference intensity ratio (RIR) is used on many occasions from the ICDD database. The RIR value from the ICDD database is a previously determined number that has been calculated through a comparison of an individual mineral with corundum or, in the GSC XRD laboratory, through a comparison with quartz (for many common silicates). At the GSC, selected minerals were prepared according to the procedure for X-ray diffraction analysis using various proportions of quartz with each powder mount that was created. These proportions usually measured 0%, 25%, 50% and 75% quartz. The JADE program was then used to determine these proportions based on the XRD patterns. In this manner, a quantitative analysis for the varying ratios of quartz/mineral could be made, and these used to establish an average RIR for the minerals in question. The RIR values created and those from the ICDD database are stored digitally in a user file that also contains minerals from the ICDD database.

The data collected generally have errors of less than 5% when the minerals are present as major phases in the rock and are matched to quartz or corundum. Errors are larger for minerals present in minor or trace amounts. Higher errors can also may occur due to a lack of predetermined RIR ratios with quartz or corundum. The mode for several mineral groups (e.g., amphiboles, garnets, biotite-pholgopite) can be reported only in their entirety (i.e., if two amphiboles are present in a sample, the Jade program can only calculate the mode as if they were only one mineral).

APPENDIX B – SAMPLE DESCRIPTIONS

See accompanying CD-ROM.

Table 3. Mode based on X-ray diffractometry[1] for Ruttan mine horizon and Derrol Lake horizon samples.

Sample No.	Distance[2] (km)	Quartz	Siderite	Dolomite	Aragonite	Calcite	Sum Carbonate	Anhydrite	Muscovite	Cordierite	Biotite	Phlogopite	Clinochlore	Clinochlore-Fe
Exhalite samples, Ruttan mine trend:														
RUT-1	-2.50	28.5				2.6	2.6				7.6		1.1	
RPE91-6-3085	0.70	33.4					0.0		7.2					
RPE89-3-1630	1.50	39.2					0.0	1.0	10.4					
RUT-15	2.95	33.6					0.0				5.9			4.2
RUT-16	3.10	58.1					0.0				4.1		2.0	
RUT88-117	53.20	40.3					0.0				5.3			2.1
RUT89-90	55.90	41.4					0.0				5.2			2.1
RUT79-107	56.40	12.0					0.0							1.4
RUT86-103	57.20	35.2					0.0				5.9			2.2
RUT85-83	59.30	46.5					0.0				15.6			1.3
RUT87-110	69.30	48.2					0.0		10.4				2.6	
RUT80-68	75.50	41.5					0.0				10.3			
Intermediate volcaniclastic samples, Ruttan mine trend:							0.0							
RUT-2	-0.50	10.6	1.1				1.1						1.2	
RUT-3	-0.20	25.9				3.1	3.1	1.4						
RUT-4	-0.10	13.9					0.0				3.5			
RUT-5	0.25	15.0					0.0					10.0		
RUT-6	0.65	27.9					0.0			6.2		9.7		
RUT-7	1.10	15.3					0.0					10.5		
RUT-8	1.25	25.4					0.0			2.3	6.8		1.4	
RUT-9	1.55	38.3					0.0				8.0		1.0	
RUT-10	1.75	16.2					0.0				7.0			
RUT-11	1.90	33.7					0.0			2.5	6.0			2.3
RUT-12	2.22	8.2					0.0			2.2				1.3
RUT-13	2.50						0.0			3.2				
RUT-14	2.80	24.4					0.0					3.9		2.3
RUT-17	3.10	24.1					0.0					3.5		
RUT78-20	29.30	72.3					0.0		11.3					3.6
RUT89-124	55.90	51.0					0.0				18.6			
RUT89-65	55.90	34.0					0.0					28.3		
RUT79-204	56.40	30.3					0.0					9.6		
RUT79-233	56.40	26.9					0.0					22.9		
RUT86-121	57.20	37.5					0.0					23.1		
RUT86-48	57.20	34.6					0.0					23.5		
RUT85-105	59.30	26.0					0.0					27.4		
RUT85-27	59.30	51.6					0.0				8.6			
RUT87-140	69.30	58.7					0.0				10.3			
RUT87-60	69.30	73.4					0.0				10.1			
Exhalite samples, Derrol Lake trend:														
RUT4-235	-2.80						0.0						1.7	
RUT15-160	-2.49	82.5					0.0			8.0	5.1			
RUT8-302	-2.44	44.1					0.0							2.3
RUT8-200	-1.78	22.9					0.0			5.9	3.7			
RUT11-185	-1.00	28.3					0.0				2.8			
RUT12-190	-0.73	35.2		2.6			2.6						2.4	
RUT13-138	-0.49	24.3					0.0		8.5					
RUT46-610	-0.34	14.8					0.0					12.1		1.8
RUT22-380	-0.12	12.5					0.0							5.0
RUT20-240	0.07	42.3	1.7	9.8		3.6	15.1				7.4			2.6
RUT23-420	0.22	57.1					0.0				12.2		1.9	
RUT26-187	2.07	33.1					0.0				5.0			1.4
RUT28-260	2.29	45.1					0.0				6.4			2.8
RUT32-220	3.48	49.8					0.0				6.3			4.1
RUT33-135	4.66	59.4					0.0				10.7			4.3
Intermediate volcaniclastic samples, Derrol Lake trend:														
RUT4-35	-2.80						0.0							
RUT15-310	-2.49	62.0					0.0	1.6				7.0		
RUT8-435	-2.44	39.7					0.0				5.9			
RUT8-60	-2.44	51.8					0.0				7.0			
RUT8-320	-1.78	46.7					0.0				5.7			2.1
RUT8-40	-1.78						0.0		11.6					15.4
RUT11-380	-1.00	13.0					0.0					18.6		
RUT11-70	-1.00	53.9					0.0				8.3			
RUT12-350	-0.73	12.4					0.0					6.8		2.2
RUT12-70	-0.73	12.2					0.0				3.9			
RUT13-35	-0.49	46.4					0.0				5.0			
RUT46-520	-0.34	56.1					0.0				8.0			
RUT46-685	-0.34	50.7					0.0				6.0			3.9
RUT22-150	-0.12	46.8					0.0				5.0			
RUT22-700	-0.12	44.1					0.0					8.1		
RUT45-55	-0.12	66.2					0.0				19.4			2.5
RUT47-120	-0.12	21.4					0.0			4.0		26.2		
RUT20-15	0.07	50.1					0.0	1.3			4.6			2.1
RUT20-450	0.07													
RUT44-35	0.07	37.5					0.0				10.5		1.0	
RUT23-670	0.22	46.5					0.0				7.7			
RUT49-45	0.22	40.9					0.0				10.2			
RUT26-120	2.07	58.4					0.0		6.7					3.2
RUT28-460	2.07	46.5					0.0				9.0			
RUT28-450	2.29	48.2					0.0					9.2		
RUT28-60	2.29	22.8					0.0					12.6		
RUT32-160	3.48	47.7					0.0				3.4			2.1
RUT32-380	3.48	46.6					0.0				3.5			3.7
RUT33-110	4.66	60.6		2.4			2.4					9.1		
RUT33-390	4.66	36.7					0.0				9.9			

[1] see Appendix A for methodology

[2] along strike from Ruttan mine or DAR2 zone

Forsterite	Albite	Albite-Ca	Orthoclase	Microcline	Almandine	Grossular	Pyrope	Sum Garnet	Kyanite	Cummingtonite	Hornblende	Actinolite	Edinite	Sum Amphibole
	40.9							0.0						0.0
		3.5		4.0				0.0				7.4		7.4
	7.9			13.4			3.4	3.4						0.0
	38.5			9.2	4.2			4.2						0.0
		8.6	4.2		4.3			4.3	11.9					0.0
	8.8							0.0				18.0		18.0
			7.3			1.6		1.6			8.3			8.3
			0.6					0.0					36.3	36.3
	11.4							0.0				18.1		18.1
		13.4						0.0						0.0
	6.2							0.0						0.0
	6.3							0.0						0.0
	20.6			2.1	1.3			1.3				56.9		56.9
		22.6	6.5					0.0				36.1		36.1
		29.9	2.1					0.3				45.1		45.1
	15.7		3.1		3.0			3.0				45.6		45.6
		19.5		12.9				0.0			9.3			9.3
	20.6							0.0				50.6		50.6
	27.1				2.5			2.5			16.7			16.7
		20.5	1.5					0.0	4.1			19.0		19.0
	21.3							0.0					44.8	44.8
		26.4			5.3			5.3			10.3			10.3
5.7	17.4			7.6				0.0				56.6		56.6
		16.7	2.1					0.0				71.0		71.0
17.0	33.9							0.0	Trace		18.4			18.4
	22.1		5.4		3.0			3.0	31.0		10.8			10.8
	9.2							0.0						0.0
	15.7			4.1	5.4			5.4						0.0
		21.0			5.1	4.8		9.9						0.0
12.1		42.7					5.4	5.4						0.0
	25.2			6.2		6.3		6.3	6.3					0.0
		32.1				4.9		4.9						0.0
		31.5				6.3		6.3						0.0
	20.2		3.1			7.2		7.2						0.0
	36.1							0.0						0.0
		21.5	4.1					0.0						0.0
	12.5							0.0						0.0
					5.0			5.0		58.6				58.6
								0.0						0.0
				3.2	3.5			3.5			4.9			4.9
10.4				5.1				0.0		50.7				50.7
13.9								0.0		23.9				23.9
		3.3		2.1				0.0		27.8				27.8
			6.6					0.0			8.2			8.2
	6.9			5.3		3.1		3.1				7.6		7.6
								0.0		25.9				25.9
	10.8			8.7			5.8	5.8	14.5		2.3			2.3
	7.2							0.0					11.2	11.2
			1.5					0.0		10.5				10.5
	8.1		2.3					0.0		10.2				10.2
						1.4		1.4		22.8				22.8
	5.1							0.0						0.0
								0.0						
								0.0						0.0
				13.0	5.8			5.8						0.0
7.1	34.1		2.5				6.3	6.3						0.0
7.7	22.6				4.5			4.5						0.0
	35.4		9.7					0.0	Trace					0.0
	16.6				3.9			3.9		43.8				43.8
8.0	36.3	36.4			3.5			3.5			9.0	26.6		35.6
	27.0						5.8	5.8	Trace					0.0
		55.3			5.0			5.0		18.2				18.2
12.3		40.6			4.5			4.5		20.9				20.9
9.6	16.9			10.2	3.9			3.9						0.0
				20.5	6.2			6.2						0.0
	23.6		8.0					0.0						0.0
10.2	10.9			18.7	3.2			3.2						0.0
	12.3			30.8				0.0						0.0
					7.0			7.0						0.0
		32.2	8.0					0.0						0.0
	20.6		8.9					0.0						0.0
								0.0						0.0
12.4	28.5				4.5			4.5						0.0
	40.0				3.2			3.2						0.0
	25.2			18.1		3.9		3.9						0.0
	13.5			11.9			6.4	6.4						0.0
	34.5				5.4			5.4						0.0
	23.8			5.2			9.6	9.6						0.0
	28.2							0.0			21.5			21.5
	35.8		8.7					0.0						0.0
	19.7		19.0				4.5	4.5						0.0
	24.7							0.0						0.0
		8.0		11.4				0.0	8.8	16.1				16.1

Pyrite	Pyrrhotite	Sphalerite	Galena	Marcasite	Chalcopyrite	Sum Sulphide	Magnetite	Hematite	Ilmenite	Titanite	Anatase	Rutile
8.4	2.7					11.1	8.2					
44.5						44.5						
12.8	5.9					18.5				6.3		
	2.8					2.8				1.7		
						0.0				6.8		
	22.1					22.1		3.2				
14.2	18.8	1.1				34.1						
8.7	16.6				24.3	49.6						
5.8	21.5					27.3						
10.4	9.0					19.4						3.7
	34.5					34.5						
	41.9					41.9						
						0.0				6.1		
				0.6		0.6						3.6
7.1						7.1						
	1.6					1.6		8.0				
10.6	3.9					14.5						
	1.5					1.5						1.8
15.1	2.7					17.8						
3.0	3.0			1.6		7.6						
8.6	2.2					10.8						
10.9						10.9			2.6			
						0.0						1.0
						0.0		5.5				
						0.0						
						0.0						
	3.5					3.5						
	5.3					5.3						Trace
	2.0					2.0						4.7
						0.0						
						0.0						6.6
	2.3					2.3						
	4.1					4.1						
	1.8					1.8	8.9					3.4
	3.5					3.5						
	5.4					5.4						
	4.1					4.1						
	24.2		3.2			27.4			7.0			
	4.4					4.4						
6.0	27.1					33.1						
	3.2					3.2			5.6			
	18.0					18.0			6.3			
5.9	2.2					8.1				6.9		
9.4	40.5					49.9						
4.3	41.1	0.2			2.8	48.4						
3.0	16.8	9.0			20.0	48.8						1.1
60.2	2.4	2.8				65.4	10.1			8.1		
	5.9	2.1				8.0	2.5					
	8.4					8.4	30.9					
8.9	18.2					27.1						
	11.2					11.2			4.4			
13.8	4.9	1.7				20.4						
						0.0						
						0.0				10.2		
						0.0				Trace		
3.8	2.5					6.3						
						0.0						
			3.5			3.5				Trace		
						0.0						
						0.0				5.1		
						0.0						
	2.8					2.8			2.8			
	2.2					2.2				5.8		
						0.0						
	2.9					2.9				5.0		
	3.0				2.2	5.2						
	4.6					4.6						
	4.1					4.1						
	6.4					6.4						1.8
						0.0				12.5		
						0.0						
	3.7					3.7						2.1
	2.7					2.7						
	1.7					1.7						
						0.0						
	2.6					2.6						
	3.2					3.2						
	5.1					5.1			5.2		0.8	
	2.3					2.3				Trace		
						0.0					3.1	
	3.2					3.2				Trace		
	2.9				4.5	7.4						1.8

Comments
Second amphibole (ferrogedrite) present
1.3% stilpnomelane?
(Unknown peak at 1.73 A)
Two micas, two amphiboles and possibly garnets present
Two amphiboles present
Two amphiboles (+ferrotschermakite?) present, two micas present
Two amphiboles (+ferrotschermakite) present
1.5% chloritoid
Two amphiboles (+ferroactinolite)
Two amphiboles (+ferrotschermakite 4-8%); kyanite probably too high
Two amphiboles present
Two micas present
Two micas present
Two micas (+muscovite)
Significant amounts of ferroglaucophane present
2.4% stilbite
Second amphibole present
Second amphibole present
4.4% diopside?
5.3% stilbite
6.3% aegerine?
4-8% of a second amphibole
~10% second amphibole present
Two micas present
Trace epidote
Second amphibole present

Table 4. Metal and trace-element contents for exhalite samples.

Sample No.	Distance Along Strike (km)	S	Cu	Zn	Zn	Pb	Au	Ag	As	Ni	Cd	Mn	Ba	Co	Cr	Fe	Na	Sc
	Units:	%	ppm	ppm	ppm	ppm	ppb	ppm	ppm	ppm	ppm	ppm	ppm	ppm	ppm	%	%	ppm
	Method:[1]	ICP	ICP	INAA	ICP	ICP	INAA	ICP	INAA	ICP	ICP	ICP	INAA	INAA	INAA	INAA	INAA	INAA
Ruttan trend:																		
RUT-1	-2.50	0.960	55	-50	48	7	-2	-0.3	1.9	2	-0.3	979	310	15	1	7.33	2.08	36.4
RPE91-6-3065	0.70	15.119	151	3530	3752	298	12	3.1	56.5	13	11.6	355	290	11	1	14.9	0.68	11.6
RPE89-3-1630	1.50	4.573	82	607	620	255	558	63.2	40.3	12	-0.3	2528	2100	26	12	6.54	0.48	25.2
RUT-15	2.95	0.258	33	270	210	42	-2	0.6	1.9	47	-0.3	1034	470	22	62	5.51	3.1	19.8
RUT-16	3.10	0.805	89	169	161	25	22	0.8	3.7	12	-0.3	1125	660	7	10	4.15	0.48	13.7
RUT88-117	53.20	9.243	841	182	254	14	3	1.5	4.3	280	0.8	3155	250	92	100	18.9	0.53	10.4
RUT89-90	55.90	9.056	408	90	87	-3	-2	1.0	11.6	126	0.8	1177	300	62	92	17.6	0.26	26.3
RUT79-107	56.40	11.189	53120	3380	3371	-3	88	4.7	-0.5	811	7.8	1419	-50	1030	106	23.4	0.03	2.2
RUT86-103	57.20	7.801	227	230	197	11	-2	0.9	2.5	185	1.2	1117	290	36	72	16	0.49	22
RUT85-83	59.30	4.342	273	92	127	7	-2	0.7	2.4	108	-0.3	628	310	22	521	9.27	1.35	15.5
RUT87-110	69.30	10.752	1072	91	48	11	33	1.6	3.6	166	1.4	269	270	59	84	27.5	0.32	6.6
RUT80-68	75.50	13.592	409	96	130	23	19	1.4	6.2	145	-0.3	1262	220	40	65	26.3	0.26	8.9
Darrol Lake trend:																		
RUT4-235	-2.80	11.158	1512	757	717	9	6	1.1	1.2	14	2.7	660	-50	22	10	34.1	0.04	0.4
RUT15-160	-2.49	1.126	2932	5740	3705	139	231	3.3	1010	10	9.7	806	180	18	42	5.59	0.13	5.4
RUT6-302	-2.44	10.709	413	2500	1281	889	29	1.5	5380	31	2.7	516	-50	37	58	25.2	0.05	1.6
RUT8-200	-1.78	3.054	75	620	465	666	9	1.5	12	4	2.6	819	-50	3	9	20.3	0.1	1.7
RUT11-185	-1.00	6.977	1203	3900	2948	122	5	1.3	2.9	8	10.1	987	-50	5	16	21.9	0.16	2.2
RUT12-190	-0.73	1.340	2007	10600	3707	40	15	2.0	5.5	15	6.3	2193	-50	7	20	13.3	0.24	4.6
RUT13-138	-0.49	9.007	271	250	210	26	5	3.2	3.4	10	3.0	957	210	2	-5	25	0.25	4.4
RUT46-610	-0.34	11.639	414	332	214	70	-2	6.0	2.9	9	0.5	1840	-50	-1	6	24.4	0.31	3.6
RUT22-380	-0.12	12.411	39950	39200	31540	746	1980	43.0	20	22	118.0	2066	-50	15	7	28.3	0.02	1.2
RUT20-240	0.07	17.542	3184	4160	3750	62	54	8.1	59	9	10.9	2442	-50	6	12	28.1	0.12	1.7
RUT23-420	0.22	2.297	461	10300	10080	2816	15	7.3	3.7	2	22.0	1270	260	3	-5	6.19	0.4	5
RUT26-187	2.07	3.974	44	339	325	41	-2	0.7	3.1	3	0.4	1354	110	3	9	19.3	0.19	0.9
RUT28-260	2.29	7.732	29	151	115	39	12	1.0	3	8	0.6	957	98	4	33	16.7	0.44	4.8
RUT32-220	3.46	4.572	166	580	571	36	40	1.0	3.1	3	1.2	2153	210	2	8	15.9	0.42	1.4
RUT33-135	4.66	3.340	932	6580	5829	21	-2	1.0	3.1	12	21.4	738	140	7	17	8.9	0.3	2.4
Duplicates, standards:																		
RPR91-6-3065 (PULP-DUP)		14.299	146	3500	3521	265	15	2.9	56.2	19	9.5	339	280	10	-5	14.7	0.68	11.8
RUT28-260 /DUP		7.770	30		112	48		1.3		10	-0.3	966						
DMMAS-18-1222				235			524		2090				450	62	143	8.18	0.78	20.1
DMMAS-18-1221				221			538		2190				430	64	145	8.32	0.75	20.4
DMMAS-18-1220				258			534		2130				420	63	152	8.52	0.8	21.4
Accepted Value-DMMAS-18B				250+/-50			544+/-72		2020+/-224				435+/-150	58+/-15	151+/-20	8.05+/-0.85	0.74+/-0.48	20.5+/-3.4

[1]analyses by Activation Laboratories, Ancaster, Ontario: INAA, neutron activation on 20-40 gm samples; ICP, 'near total' digestion by multi-acid attack and inductively coupled plasma spectrometric analysis

Se	Th	U	La	Ce	Nd	Sm	Eu	Eu*	Tb	Yb	Lu	Al	Ca	K	Mg	P	Sr	Ti	V	Y
ppm	ppm	ppm	ppm	ppm	ppm	ppm	ppm		ppm	ppm	ppm	%	%	%	%	%	ppm	%	ppm	ppm
INAA	INAA	INAA	INAA	INAA	INAA	INAA	INAA	INAA	INAA	INAA	INAA	ICP	ICP	ICP	ICP	ICP	ICP	ICP	ICP	ICP
-3	2.8	-0.5	8.2	16	-5	1.9	0.7	0.98	-0.5	1.4	0.21	5.68	4.45	1.14	0.79	0.075	270	0.64	191	8
-3	3.4	1.1	15.8	29	10	4.1	0.9	0.58	0.6	4.3	0.64	4.82	1.39	1.13	1.72	0.038	99	0.10	21	15
-3	1.9	1	7	13	-5	2.1	0.9	1.14	-0.5	2.9	0.44	5.60	1.39	5.73	0.78	0.049	49	0.25	150	13
-3	8.8	2.2	56.2	98	41	9.1	2.1	0.61	-0.5	2.4	0.37	5.92	1.34	3.13	2.10	0.130	518	0.44	115	22
-3	3.8	2	11.7	27	6	3	0.8	0.71	-0.5	4.3	0.66	3.62	1.18	3.20	0.50	0.023	68	0.19	38	19
17	7.9	5.9	36	67	20	6.4	1.3	0.54	0.8	3	0.45	3.49	2.74	1.13	2.15	0.247	98	0.22	289	43
-3	2.7	3.7	13.8	23	14	3.3	0.9	0.73	-0.5	2.5	0.41	3.55	3.29	0.63	1.53	0.071	94	0.48	252	28
-3	-0.2	2.9	2.5	3	-5	0.5	-0.2	0.50	-0.5	0.3	0.05	0.55	2.82	0.16	3.81	0.009	16	0.04	38	5
-3	1.8	3.5	10.3	19	9	3	0.8	0.71	-0.5	2.3	0.35	3.59	3.34	1.01	1.62	0.071	160	0.34	166	17
-3	4.8	9.2	17.8	33	14	3.2	0.7	0.58	-0.5	2	0.3	4.65	1.18	2.89	2.53	0.065	153	0.21	158	13
11	7.1	4.7	23.5	39	15	3.6	0.6	0.44	-0.5	1.3	0.23	2.52	0.30	1.45	0.31	0.075	33	0.13	258	8
-3	6.9	3.5	24.4	42	15	4	0.5	0.33	-0.5	2.9	0.46	2.73	0.48	1.73	1.60	0.082	39	0.16	153	14
79	0.3	-0.5	10.3	17	9	2.2	0.6	0.73	-0.5	1.4	0.21	0.32	0.67	-0.01	6.22	0.259	8	-0.01	6	21
19	2.9	1	23	43	14	5.2	1.2	0.61	0.8	4.5	0.67	3.35	2.04	0.74	2.53	0.122	53	0.10	32	22
-3	2	2.3	11.6	25	-5	2.8	1	0.95	-0.5	2.1	0.32	0.60	0.79	0.06	1.88	0.155	9	0.04	18	19
4	0.7	-0.5	13	29	13	3.5	0.6	0.46	-0.5	3.1	0.47	1.26	0.36	0.04	5.27	0.109	11	0.05	11	17
11	0.9	1.3	14.7	28	10	3.6	0.6	0.44	0.6	3.6	0.56	1.63	1.33	0.33	4.85	0.164	16	0.05	24	29
11	2.5	1.3	24.4	50	22	6.6	1.1	0.44	1	7.4	1.17	3.54	1.30	0.28	2.67	0.138	38	0.15	45	63
-3	1.6	2	21.2	43	19	6	2.3	1.02	1.1	8.4	1.24	2.48	3.29	1.24	2.79	0.091	28	0.08	5	24
-3	2.7	2.2	22	43	19	6	15.2	6.74	1	6.2	0.9	2.52	3.85	1.29	2.62	0.073	56	0.13	4	34
34	-0.2	1.9	7.3	13	8	1.9	2	2.80	-0.5	1.6	0.24	0.79	0.87	0.02	2.44	0.252	11	0.04	15	21
7	0.8	1.4	9.6	19	5	2.6	2.3	2.35	-0.5	3.3	0.48	1.04	8.33	0.06	5.73	0.105	29	0.04	4	33
-3	3.1	1.8	26.2	58	23	7.7	2.1	0.73	1.4	11.1	1.63	4.62	1.78	2.20	2.65	0.017	72	0.15	3	35
3	1.7	1.5	20.5	37	12	4.9	0.9	0.49	0.7	5.8	0.86	2.13	0.29	1.23	2.09	0.074	12	0.04	4	15
-3	1.9	1.3	29.9	55	26	7.3	1.2	0.44	1.1	5.3	0.79	2.29	0.87	0.93	2.20	0.070	53	0.06	19	30
-3	2.6	1.8	19.4	40	17	5.2	1.2	0.61	0.9	7	1.09	2.98	1.29	0.85	2.63	0.110	52	0.07	4	42
6	3	1.4	24.5	53	21	6.9	1.7	0.66	1.1	6.7	1.08	2.61	0.71	0.88	1.66	0.107	67	0.08	13	38
-3	3.6	1.3	15.4	28	11	4.2	0.9		-0.5	4.4	0.66	4.54	1.31	1.05	1.57	0.037	95	0.09	19	16
												2.38	0.89	0.94	2.05	0.072	56	0.07	20	30
-3	-0.2	-0.5	11.6	20	11	4	1.1		-0.5	3.5	0.53									
-3	1	-0.5	12	21	12	3.9	1.1		-0.5	3.6	0.54									
-3	1.4	-0.5	12	21	10	4	1.3		-0.5	3.7	0.54									
	1.5+/-0.5		12.2+/-1.3	23+/-3	11+/-3	4.1+/-0.5	1.2+/-0.2		0.8+/-0.35	3.6+/-0.6	0.54+/-0.05									

Appendix B - Sample Descriptions

Sample No.[1]	Distance[2] (km)	General Location	Analysis	Description
RUT-1	-2.50	Ruttan mine area	XRD+Metals	Intermediate to felsic ash tuff/volcaniclastic, 30% pyrite
RUT-2	-0.50	Ruttan mine area	XRD	Intermediate ash tuff, moderate chlorite alteration; within lapilli tuff/agglomerate, blocky juvenile and probably exotic fragments, crystal ash matrix
RUT-3	-0.20	Ruttan mine area	XRD	Intermediate ash tuff, moderate to strong chlorite alteration, possible staurolite
RUT-4	-0.10	Ruttan mine area	XRD	Intermediate ash tuff, moderate to strong chlorite alteration, possible staurolite
RUT-5	0.25	Ruttan mine area	XRD	Well bedded intermediate crystal ash tuff/phyllite
RUT-6	0.65	Ruttan mine area	XRD	
RPE91-6-3065	0.70	Ruttan mine area	XRD+Metals	Sericite-pyrite schist, minor garnet, cordierite, 3-7% pyrite, chalcopyrite, pyrrhotite,
RUT-7	1.10	Magazine #1 shed	XRD	Intermediate ash tuff with slight chlorite alteration; within interbedded crystal ash tuff and
RUT-8	1.25	Magazine #4 shed	XRD	Intermediate ash and crystal ash tuff, 1% pyrite, slight silicification along fractures
RPE89-3-1630	1.50	Ruttan mine area	XRD+Metals	Intermediate ash tuff, 2-5% pyrite and pyrrhotite
RUT-9	1.55	NW 300m from Mag. #4	XRD	Intermediate ash and crystal ash tuff, 1% pyrite, slight silicification along fractures
RUT-10	1.75	NW 550m from Mag. #4	XRD	Intermediate ash and crystal ash tuff, 1% pyrite, slight silicification along fractures
RUT-11	1.90	East of Ruttan mine area	XRD	Well bedded intermediate volcaniclastic ?crystal ash tuff, slight silicification along fractures
RUT-12	2.22	East of Ruttan mine area	XRD	Intermediate volcaniclastic/schist, slight silicification
RUT-13	2.50	East of Ruttan mine area	XRD	Intermediate ash tuff/volcaniclastic/schist, slight epidote alteration and silicification
RUT-14	2.80	East of Ruttan mine area	XRD	
RUT-15	2.95	East of Ruttan mine area	XRD+Metals	
RUT-16	3.10	East of Ruttan mine area	XRD+Metals	Siliceous intermediate ash tuff/exhalite, 5% pyrite
RUT-17	3.10	East of Ruttan mine area	XRD	Intermediate ash crystal tuff
RUT78-20	29.30	East of Rat River	XRD	Intermediate ash tuff/volcaniclastic/schist, with chlorite and tremolite-actinolite
RUT88-117	53.20	East of Rat River	XRD+Metals	Intermediate fine-grained volcaniclastic/graywacke/phyllite
RUT89-124	55.90	East of Rat River	XRD	Intermediate ash tuff/schist, trace epidote
RUT89-65	55.90	East of Rat River	XRD	Intermediate fine-grained volcaniclastic/graywacke/phyllite
RUT89-90	55.90	East of Rat River	XRD+Metals	Intermediate schist with 15% pyrite and pyrrhotite, 1-3% garnet
RUT79-107	56.40	East of Rat River	XRD+Metals	Semi-massive sulfide, 30% pyrrhotite+pyrite, 2% chalcopyrite in intermediate volcanic, moderate chlorite alteration, possible minor cordierite
RUT79-204	56.40	East of Rat River	XRD	Well layered intermediate schist/gneiss
RUT79-233	56.40	East of Rat River	XRD	Intermediate ash tuff/volcaniclastic/schist, with chlorite and tremolite -actinolite
RUT86-103	57.20	East of Rat River	XRD+Metals	Semi-massive sulfide, 25% pyrit+pyrhotite and minor chalcopyrite, within intermediate to
RUT86-121	57.20	East of Rat River	XRD	Intermediate ash tuff/metapelite
RUT86-48	57.20	East of Rat River	XRD	Intermediate ash tuff/metapelite
RUT85-105	59.30	East of Rat River	XRD	
RUT85-27	59.30	East of Rat River	XRD	Intermediate ash tuff/metapelite
RUT85-83	59.30	East of Rat River	XRD+Metals	Intermediate ash tuff/metapelite, 5% pyrrhotite and pyrite
RUT87-110	69.30	East of Rat River	XRD+Metals	Massive sulfide, with 50% pyrrhotite+pyrite and trace chalcopyrite, within intermediate ash
RUT87-140	69.30	East of Rat River	XRD	Well layered intermediate ash tuff, trace pyrite along fractures
RUT87-60	69.30	East of Rat River	XRD	Intermediate ash tuff/schist, trace epidote
RUT80-68	75.50	East of Rat River	XRD+Metals	Semi-massive sulfide, 25% pyrrhotite+pyrite, trace chalcopyrite and sphalerite in intermediate schist with moderate chlorite alteration
RUT4-235	-2.80	Dar1 Zone Area	XRD+Metals	Semi-massive sulfide, predominantly pyrrhotite and pyrite, chlorite, muscovite, ?tremolite-
RUT4-35	-2.80	Dar1 Zone Area	XRD	Intermediate ash tuff, slight silicification along fractures

RUT15-160	-2.49	Dar1 Zone Area	XRD+Metals	Intermediate ash tuff/volcaniclastic, 5% pyrite and pyrrhotite, 1+% magnetite, with trace
RUT15-310	-2.49	Dar1 Zone Area	XRD	Intermediate ash tuff/volcaniclastic
RUT6-302	-2.44	Dar1 Zone Area	XRD+Metals	Semi-massive sulfide, 30% pyrrhotite and pyrite, ?5% garnet
RUT6-435	-2.44	Dar1 Zone Area	XRD	Intermediate ash tuff, probably moderate sodium depletion, schistose, strong lineation
RUT6-60	-2.44	Dar1 Zone Area	XRD	Intermediate ash tuff, trace pyrite along fractures
RUT8-200	-1.78	Dar1-Dar2	XRD+Metals	
RUT8-320	-1.78	Dar1-Dar2	XRD	
RUT8-40	-1.78	Dar1-Dar2	XRD	Well layered intermediate ash tuff/volcaniclastic
RUT11-185	-1.00	Dar1-Dar2	XRD+Metals	Sulfidic intermediate ash tuff, 20% pyrite and pyrrhotite, 3% garnet, possible hornblende
RUT11-360	-1.00	Dar1-Dar2	XRD	Well laminated intermediate ash tuff/volcaniclastic
RUT11-70	-1.00	Dar1-Dar2	XRD	
RUT12-190	-0.73	Dar1-Dar2	XRD+Metals	Garnet chlorite schist with 2-5% pyrite and pyrrhotite
RUT12-350	-0.73	Dar1-Dar2	XRD	Intermediate ash tuff/volcaniclastic, with tremolite-actinolite
RUT12-70	-0.73	Dar1-Dar2	XRD	Intermediate ash tuff/volcaniclastic, moderate chlorite alteration, with tremolite-actinolite
RUT13-138	-0.49	Dar1-Dar2	XRD+Metals	Intermediate sulfidic ash tuff, 15% pyrite and pyrrhotite, with amphibole (termolite-actinolite
RUT13-35	-0.49	Dar1-Dar2	XRD	Well bedded intermediate ash tuff/volcaniclastic
RUT46-520	-0.34	Dar2 Zone Area	XRD	Intermediate ash crystal tuff, moderate sodium depletion, incipient garnet, schistose
RUT46-610	-0.34	Dar2 Zone Area	XRD+Metals	Semi-massive sulfide, 35% pyrrhotite, pyrite, minor chalcopyrite, sphalerite, with garnet,
RUT46-685	-0.34	Dar2 Zone Area	XRD	Well layered intermediate ash tuff, slight chlorite alteration, with tremolite-actinolite, trace
RUT22-150	-0.12	Dar2 Zone Area	XRD	Intermediate-felsic ash crystal tuff, trace pyrite
RUT22-380	-0.12	Dar2 Zone Area	XRD+Metals	semi-massive sulfide: 20-40% pyrite-pyrrhotite-chalcopyrite-sphalerite in altered
RUT22-700	-0.12	Dar2 Zone Area	XRD	Intermediate-felsic ash crystal tuff/volcaniclastic, well bedded
RUT45-55	-0.12	Dar2 Zone Area	XRD	Intermediate ash tuff, trace pyrite
RUT47-120	-0.12	Dar2 Zone Area	XRD	Intermediate ash tuff, well laminated, slight-moderate chlorite alteration, with tremolite-
RUT20-15	0.07	Dar2 Zone Area	XRD	Felsic-intermediate crystal ash tuff
RUT20-240	0.07	Dar2 Zone Area	XRD+Metals	Sulfide-rich altered intermediate ash tuff
RUT20-450	0.07	Dar2 Zone Area	XRD	Felsic-intermediate crystal ash tuff, 1% pyrite, trace garnet
RUT44-35	0.07	Dar2 Zone Area	XRD	Well layered intermediate ash tuff, trace epidote along fractures
RUT23-420	0.22	Dar2 Zone Area	XRD+Metals	Altered intermediate tuff with 2-5% pyrite, pyrrhotite, minor to trace chalcopyrite, sphalerite
RUT23-670	0.22	Dar2 Zone Area	XRD	Intermediate to felsic ash crustal tuff, trace pyrite
RUT49-45	0.22	Dar2 Zone Area	XRD	Well layered intermediate ash tuff, trace epidote along fractures
RUT26-120	2.07	Dar3 Zone Area	XRD	Altered intermediate schist/phyllite with garnet, muscovite, possible sillimanite, 1% pyrite
RUT26-187	2.07	Dar3 Zone Area	XRD+Metals	Siliceous pyritic felsic ash tuff/exhalite with 15% pyrite and pyrrhotite and 3% magnetite
RUT26-460	2.07	Dar3 Zone Area	XRD	Felsic ash tuff/volcaniclastic, 0.2% pyrite
RUT28-260	2.29	Dar3 Zone Area	XRD+Metals	Intermediate to felsic ash tuff/volcaniclastic with 10% pyrite and pyrrhotite, 5% fine-grained
RUT28-450	2.29	Dar3 Zone Area	XRD	Intermediate to felsic ash tuff/volcaniclastic
RUT28-50	2.29	Dar3 Zone Area	XRD	Altered intermediate tuff/volcaniclastic, with possible trace garnet, trace staurolite, tremolite
RUT32-160	3.46	Dar3 Zone Area	XRD	
RUT32-220	3.46	Dar3-Dar4	XRD+Metals	Intermediate to felsic ash tuff/volcaniclastic with 10% pyrite and pyrrhotite, 5% fine-grained
RUT32-380	3.46	Dar3-Dar4	XRD	
RUT33-110	4.66	Dar4 Zone Area	XRD	Well-bedded intermediate ash tuff, 0.3% pyrite
RUT33-135	4.66	Dar4 Zone Area	XRD+Metals	Altered intermediate ash fuff with 2-5% pyrite, pyrrhotite, chalcopyrite, trace sphalerite;
RUT33-350	4.66	Dar4 Zone Area	XRD	Well bedded intermediate ash tuff, possible incipient garnet, possible iron carbonate

[1]RUT1, etc from outcrop, the remainder from drillholes, with name reflecting DDH number and interval

[2]along strike from Ruttan mine shaft or from central DAR2 zone